Pontifícia Universidade Católica do Rio de Janeiro

Tatiana Naccache Rochinha

A study of normal stresses in shear flow of viscoplastic materials

Dissertação de Mestrado

Dissertation presented to the Programa de Pós–graduação em Engenharia Mecânica of PUC-Rioin partial fulfillment of the requirements for the degree of Mestre em Engenharia Mecânica.

Advisor : Prof. Paulo Roberto de Souza Mendes
Co-advisor: Dr. Priscilla Ribeiro Varges

Rio de Janeiro
September 2021

PONTIFÍCIA UNIVERSIDADE CATÓLICA DO RIO DE JANEIRO

Tatiana Naccache Rochinha

A study of normal stresses in shear flow of viscoplastic materials

Dissertation presented to the Programa de Pós–graduação em Engenharia Mecânica of PUC-Rioin partial fulfillment of the requirements for the degree of Mestre em Engenharia Mecânica. Approved by the Examination Committee.

Prof. Paulo Roberto de Souza Mendes
Advisor
Departamento de Engenharia Mecânica – PUC-Rio

Dr. Priscilla Ribeiro Varges
Co-advisor
Departamento de Engenharia Mecânica – PUC-Rio

Prof. Roney Leon Thompson
Programa de Engenharia Mecânica – COPPE – UFRJ

Prof. Márcio da Silveira Carvalho
Departamento de Engenharia Mecânica – PUC-Rio

Rio de Janeiro, September the 14th, 2021

Tatiana Naccache Rochinha

Tatiana Naccache Rochinha graduated in Mechanical Engineering at Pontifical Catholic University of Rio de Janeiro (PUC- Rio) in 2018. Then, she started her master's degree on rheology and non-Newtonian fluid mechanics in the Rheology Group (GReo) at PUC–Rio, where she was already involved in research activities for three years as an undergraduate student.

Bibliographic data

Rochinha, Tatiana Naccache

A study of normal stresses in shear flow of viscoplastic materials / Tatiana Naccache Rochinha; advisor: Paulo Roberto de Souza Mendes; co-advisor: Priscilla Ribeiro Varges. – 2021.
v., 93 f: il. color. ; 30 cm

Dissertação (mestrado) - Pontifícia Universidade Católica do Rio de Janeiro, Departamento de Engenharia Mecânica, 2021.
Inclui bibliografia

1. Engenharia Mecânica – Teses. 2. Reologia;. 3. Tensão normal;. 4. Forças normais;. 5. Viscoelasticidade;. 6. Materiais elastoviscoplásticos.. I. Mendes, Paulo Roberto de Souza. II. Varges, Priscilla Ribeiro. III. Pontifícia Universidade Católica do Rio de Janeiro. Departamento de Engenharia Mecânica. IV. Título.

CDD: 621

Acknowledgments

Firstly, I would like to thank my advisor Paulo Roberto de Souza Mendes for the guidance, encouragement and support in my many years in the laboratory. I deeply appreciate all the extra push to challenge me in this exciting research topic.

I would also like to acknowledge my coadvisor Priscilla Ribeiro Varges that has been a mentor and a close friend for the last couple of years. Your advice, dedication and support have guided me throughout the whole research. Without you, none of this would be possible.

I am thankful for my two closest friend, Gabi and Julia for all the support in the last 20 years. To Dani and Fernanda, as well, for being excellent friends and supporters.

I am greatful for all of my colleagues at the Rheology Group at PUC-Rio for the assistance provided in many aspects. Thank you for your advice and our technical exchange.

I would like to acknowledge speacially Eliana and Ricardo for the partnership and support in our project together. Your leadership was essential for my development and your friendship made everything a little more special.

I am thankful for Lorena for all the help in the laboratory throughout the last years and for making my time there easier, funnier and memorable. I would like to acknowledge Pedro for being a good friend in these years. Also, I would like to thank my cousin, João Pedro, for all the jokes that made our time at the laboratory lighter.

I thank Camila for being my closest friend, confidant and helper throughout these years. You made it all so much easier and wonderful. In addition, I would like to acknowledge all the help in the laboratory with the tests and graphs, for staying late and arriving early when necessary. Thank you for lifting me up and calming me down when I needed it. Finally, thank you for being my rock and my person.

To my sister, you are my biggest supporter. Thanks for always making me laugh when I needed it.

I am grateful for my parents. For their guidance, support and love always. You have made me a better person and professional by pushing and challenging me. It was amazing to follow in these enormous footsteps.

This study was financed in part by the Coordenação de Aperfeiçoamento de Pessoal de Nível Superior - Brasil (CAPES) - Finance Code 001.

Abstract

Rochinha, Tatiana Naccache; Mendes, Paulo Roberto de Souza (Advisor); Varges, Priscilla Ribeiro (Co-Advisor). **A study of normal stresses in shear flow of viscoplastic materials**. Rio de Janeiro, 2021. 93p. Dissertação de Mestrado – Departamento de Engenharia Mecânica, Pontifícia Universidade Católica do Rio de Janeiro.

This work proposes to investigate normal stress measurements for yield stress materials. Using an ARES-G2 TA Instruments' strain-controlled rheometer, three different elastoviscoplastic materials were studied. A simple but effective experimental procedure was developed to obtain repetitive results for both steady-state and transient measurements. These tests were put to comparison, and interesting results were obtained. For the Carpobol dispersion and the commercial hair gel, transient and steady-state results were quite similar. Although, the same was not observed for the highly concentrated emulsion. Also, variables such as N_1, ψ_1, τ, $\dot{\gamma}$, G', G'', η, τ_y, σ_s were explored to better understand the stress state of these materials. Furthermore, normal stresses were significantly higher than shear stresses, while all materials were submitted to low shear rates. For high shear rates, different from the other two fluids, the highly concentrated emulsion displayed normal stress values that were lower than shear stress ones. Finally, in contrast with most results found in literature, only negative normal stress results were obtained for the materials studied.

Keywords

Rheology; Normal stresses; Normal forces; Viscoelasticity; Elastoviscoplastic materials.

Resumo

Rochinha, Tatiana Naccache; Mendes, Paulo Roberto de Souza; Varges, Priscilla Ribeiro. **Estudo das tensões normais em escoamento cisalhante de materiais viscoplásticos**. Rio de Janeiro, 2021. 93p. Dissertação de Mestrado – Departamento de Engenharia Mecânica, Pontifícia Universidade Católica do Rio de Janeiro.

Esse trabalho propõe investigar medidas de tensão normal para materiais com tensão limite de escoamento. O reômetro ARES-G2 da TA Instruments de deformação controlada foi utilizado para estudar três diferentes materiais elastoviscoplásticos. Um procedimento experimental simples e efetivo foi desenvolvido para obter resultados repetitivos de medidas em regime permanente e transiente. Respostas interessantes foram obtidas mediante comparação dos resultados destes fluidos. Para a dispersão de Carbopol e o gel de cabelo, os resultados entre os testes transientes e em regime permanente foram bastante similares. Porém, o mesmo não foi observado para a emulsão altamente concentrada. Além disso, variáveis como N_1, ψ_1, τ, $\dot{\gamma}$, G', G'', η, τ_y, σ_s foram exploradas para um melhor entendimento do estado de tensão desses materiais. Ademais, as tensões normais medidas foram extremamemente mais altas que as tensões cisalhantes, quando o material foi submetido à baixas taxas de cisalhamento. Para altas taxas de cisalhamento, diferentemente dos outros dois fluidos, a emulsão altamente concentrada apresentou valores de tensão normal que eram mais baixos do que os de tensão cisalhante. Por fim, em contraste com a maioria dos resultados encontrados na literatura, apenas tensões normais negativas foram obtidas para os materiais estudados.

Palavras-chave

Reologia; Tensão normal; Forças normais; Viscoelasticidade; Materiais elastoviscoplásticos.

Table of contents

List of figures

1
Introduction

Shear induced flows in non-Newtonian fluids have been thoroughly studied for decades. Yield stress materials play a central role in this context. Recently, the effect caused by these flows in the normal direction has been given special attention.

A tensor is a linear mapping of vectors to vectors (59). The stress tensor is comprised of different components, the normal stresses, which are associated to forces perpendicular to the surface, and the shear stresses, which are asssociated to those forces that are parallel to the surface. This can be seen in figure 1.1.

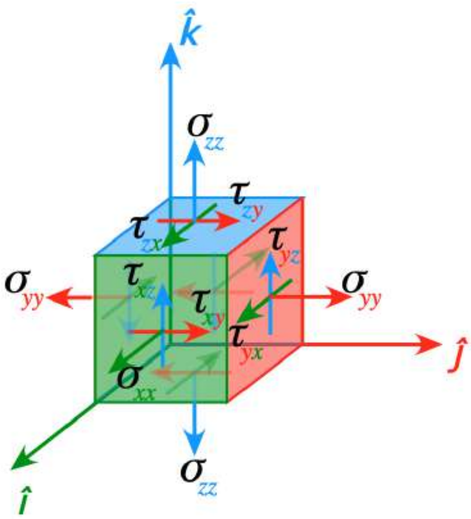

Figure 1.1: Stress tensor

When fluids are sheared between two parallel surfaces, in addition to the viscous shear stress, normal stress differences are introduced into the system: $N_1 = \sigma_{xx} - \sigma_{yy}$ and $N_2 = \sigma_{yy} - \sigma_{zz}$ (50).

In viscometric flows, the normal stress differences are equal to zero for Newtonian fluids but some non-Newtonian fluids present non zero normal stress differences. Elastic materials, polymer melts, and solutions were researched and introduced interesting findings due to the presence of normal stresses (11). Highly concentrated emulsions (55) and suspensions (**?**) under shear are now being investigated for similar behavior.

These stresses are behind many interesting phenomena such as rod climbing, die swell, and tubeless siphon (22), as well as unique rheological properties. Effects such as these can be significant for industrial and commercial applications.

Normal stresses can be sensitive to microstructural changes by process flows such as large scale disentangling of chains, drop deformation, and phase change due to shear (29). Also, the presence of stresses in the normal direction can affect the stability of shearing flows (52).

It is crucial to analyze the full tensorial stress state of a complex fluid flow in order to understand its behavior completely. An experimental study investigating both shear and normal stresses is key to developing constitutive equations that truly mimic the material's behavior under shear flows.

Recent works on viscoplastic materials reported significant magnitude of normal stresses. Below the yield stress, these materials behave as very high-viscosity elastic fluids. While at the yield stress, a microstructure collapse occurs, causing the viscosity to fall dramatically, and above the yield stress, the material presents a viscous behavior.

Elastoviscoplastic materials can be found in many industries, such as food, pharmaceutical, oil, and others. Some of them are gels, toothpaste, ketchup, emulsions, paint, and drilling fluids. In literature, many works on viscoplastic materials can be found (cf (19),(18),(8),(25)). Most of them aim to explore the many interesting phenomena surrounding shear deformation. Whereas, to fully comprehend the behavior of these complex fluids, both deformation and stress in the normal direction should also be studied.

Some recent works have shown a dependence of the material's yield stress on the normal stress, illustrating an elastic nature of yield stress (cf (22)). This work will also analyze the possible presence of a normal yield stress.

The general assumption embedded in the viscoplastic models, such as Herschel-Bulkley, Bingham, Casson, and others, is that these materials are inelastic and show no normal stress in viscometric flows (72). However, this is far from correctly predicting the fluid's behavior. This study aims to elucidate the importance of normal stresses for the stress tensor analysis used to describe the rheological characteristics of viscoplastic materials undergoing shear deformation.

Another highly accepted theory in the literature is that the Von Mises criterion applies to all soft solids (72). It is said that the elastic-to-plastic transition occurs due to the action of shear stresses and can be described by this criteria (51). Some elastoviscoplastic materials were analyzed, and despite part of them displaying normal stresses when sheared, these studies usually dismiss their presence when accounting for the Von Mises criterion (22). It is then essential to investigate the applicability of this criteria to the materials studied in this work.

Finally, the measurement of normal stresses in shear flows is extremely challenging (21). The residual normal stresses, the heterogeneity of the flow (1, 68), uncontrolled trapped strains (38), and other problems are the root of these difficulties, underlining the importance of well defined experimental protocols. To achieve accurate measurements using a strain-controlled commercial rheometer, a rigorous but simple methodology to determine normal stresses for viscoplastic materials is proposed.

1.1 Motivation

Normal stresses are present in all complex fluids. There has been considerable activity in recent years investigating their influence in the stress tensor of elastoviscoplastic materials. Yield stress fluids are ubiquitous in almost all industries, emphasizing the importance of these studies. A breakthrough in this field could be significant for industrial processes.

The behavior of these yield stress fluids under shear can be shaped by both shear and normal stresses, as shown in recent works by Thompson et al (72), de Cagny et al (22) and Habibi et al (35). These discussions elucidate the importance of the normal stresses to their full tensorial state when these elastoviscoplastic materials are submitted to shear flows.

The interest to establish invariant viscoplastic constitutive equations that can truly predict the stress tensor of yield stress materials has grown significantly over the years (22). The usual viscoplastic models erroneously present a one-to-one correspondence between the shear component of the yield stress tensor and yield stress to all elastoviscoplastic materials (72). This illustrates the importance of meaningful measurements of the components of the stress tensor other than the shear stress.

Although the interest in this field of study has risen in the last decades, not many works have managed to introduce conclusive results for viscoplastic materials. The very few measurements of normal stress in viscoplastic materials do not present an agreement regarding the sign of the normal stress differences (22). Negative N_1 has been reported for some systems (39, 58, 37), whereas others (4, 35, 66) exhibited positive values (22, 35). Furthermore, the magnitude of the first normal stress difference found in these studies varies significantly.

Some recent works (73, 72) raised a discussion that questions the applicability of the Von Mises criterion for yield stress fluids due to the presence of normal stresses. This criterion has been tested for some viscoplastic materials (31, 2), but these studies dismiss the evident existence of stresses in the normal direction (21). Recently, de Cagny et al. (22) found good agreement for the Von Mises criterion while conducting a study for elastoviscoplastic materials that displayed significant normal stresses. Thus, it is interesting to investigate the influence of these stresses on the Von Mises criterion for the materials used in this work.

However, the complexity surrounding normal stress measurements for elasto-viscoplastic materials has led to a gap in this field of study. It is important to investigate the best procedure to measure the normal stresses when the fluid undergoes steady state rheological tests under shear.

1.2 Research objectives

The present research aims to study normal stresses for different viscoplastic materials, namely a Carbopol® dispersion, a commercial hair gel, and a highly concentrated emulsion undergoing shear flows. An experimental protocol will be introduced, using a commercial strain-controlled rheometer to get meaningful normal stress measurements.

This work aims to investigate the relationship between the shear deformation and normal stresses of these yield stress materials through rheological experiments. Furthermore, the Von Mises criterion will be evaluated in order to determine if it is, in fact, applicable to the materials tested in this study. This will allow the stress tensor of these fluids to be better comprehended.

1.3 Outline

This work is divided into five chapters, including this one. The introduction, motivation, and research objectives of this research were briefly described in Chapter 1. Following, Chapter 2 includes the concepts of rheology and the definition of viscoplastic fluids. Then, the literature surrounding normal stresses is revisited and discussed.

In chapter 3, the materials chosen for this work are presented. Then, the methodology used to characterize the yield stress material is introduced. The rheological procedure developed for normal stress measurements is depicted in detail. Some of the methodology steps are better explained later in appendix A, which also integrates this chapter. The transducer validation was also described in this chapter.

Chapter 4 presents the results of the rheological characterization. Preliminary results, which showed some challenges with the measurements, are extensively discussed. The solution to this problem was a pretest procedure detailed in the appendix B.1. Lastly, the final results are presented and discussed.

Chapter 5 highlights the main conclusions of this work. Finally, future steps are suggested.

2
Background and literature

2.1
Rheology

The science of flow has been around for hundreds of years, playing an essential role in day-to-day life. The field of study concerned with the flow of matter and deformation of materials was named Rheology by Professor Bingham in the early 1900s (8). This interdisciplinary area of science is constantly pursuing the relationship between stress, strain, and time in order to characterize the fluid response to external excitations.

The term "rheometry" refers to the experimental technique developed to determine rheological properties of materials. These fluids are submitted to simple flows, such as steady shear flow, to investigate the material's behavior (8). The properties studied may be correlated to operations and processes seen in the industry. Viscosity is amongst the most important of these properties, and it is attributed to the fluid's resistance to flow (34).

Flows can be separated into two distinct groups, extensional and shear, due to the movement of the adjacent particles of the fluid, as seen in figure 2.1.

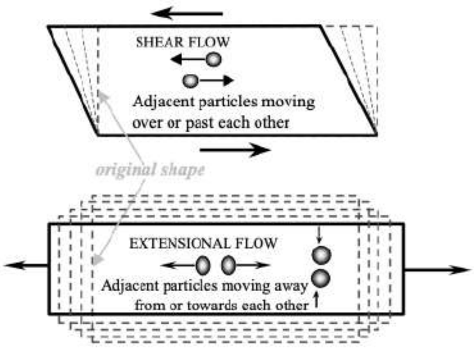

Figure 2.1: Shear and extensional flow (34)

Rheological measurements can be split into two fields: bulk rheology and interfacial rheology. The latter describes the relationship between interfacial deformation, the stresses exerted in and on it, and the resulting flows in the adjacent fluid phases (48). The main focus of this work is bulk rheology. This powerful tool is used to monitor the bulk properties of complex fluids by analyzing the deformation of these materials (34).

A rheometer is defined as an instrument used to obtain rheological properties of materials (8). The fluid studied is placed in a known geometric configuration in a controlled environment. Deformation or stress is then applied to the material, and its response is measured to provide rheometrical information. These instruments can be separated into three distinct categories, namely capillary, extensional, or rotational.

The first uses flow through a capillary tube in order to obtain the viscosity of fluids. The pressure drop and average velocity are measured to characterize the material. Capillary rheometers can achieve very high shear rates and are thus used to mimic the deformations that materials undergo in many industrial operations, such as spraying and extrusion.

Extensional rheometers investigate the behavior of fluids that undergo extensional flow. The materials are submitted to either a constant extensional strain rate or a step extensional displacement to measure their uniaxial extensional properties (61). These are pertinent to many processes such as fiber production, flow in porous media, food materials, and droplet formation.

Finally, rotational rheometers analyze how a material performs while undergoing shear deformation. These instruments, also known as shear rheometers, can be separated into stress-controlled or deformation-controlled. When materials are submitted to oscillatory experiments, stress or strain varies at an angular frequency while the storage and loss moduli are obtained. On the other hand, simple shear flow experiments can lead to the values of viscosity and coefficient of normal stresses.

A frequent test used in this field is the flow curve, in which viscosity is measured as the shear rate varies within a chosen range. This experiment investigates the apparent viscosity dependence on both shear rate and shear stress (51). Also, the dynamic yield stress can be analyzed for viscoplastic materials. In this experiment, all points are obtained in a steady-state regime.

For a stress ramp test, the rheometer imposes stress within a selected range of values to obtain the material's deformation response and its viscosity. This experiment has the same objective as a flow curve, although it is done while taking transient measurements.

A peak hold test examines, over a selected time, the behavior of the stress of the material while it undergoes constant shear rate, whereas in a creep test, the stress is constant, and its shear rate response is evaluated. The value of the material's static yield stress can be obtained with precision. Also, thixotropy can be studied as well.

A stress step change is a creep test for a selected shear stress value, followed by a second creep test with a new shear stress value. Firstly, the sample is submitted to a stress value for a selected time, and then the fluid is subjected another stress value for another chosen amount of time. This test is useful for assessing the elasticity of the yielded material and for providing the time required for the microstructure to rebuild (74).

Stress sweeps are oscillatory tests where applied shear stress amplitude varies through a chosen range while the frequency remains at a fixed value. This test allows us to examine how the loss modulus (G") and the storage modulus (G’) vary as a function of stress amplitude, leading to the definition of the viscoelastic linear region, where both elastic and viscous effects are present. Further, it is possible to determine which behavior will be more influential in a chosen state.

Another powerful rheology tool is a frequency sweep test. In this experiment, the loss modulus (G") and the storage modulus (G’) are analyzed as a function of frequency in the viscoelastic linear region. In frequency sweep tests, measurements are performed at constant strain amplitude while varying the frequency magnitude. This analysis is usually done to describe the time-dependent behavior of a sample in the non-destructive deformation range.

Finally, time sweep is a critical test to perform. This test is used to establish the time dependant structural effects for a specific stress amplitude by analyzing the loss and the storage moduli. Additionally, material stability, sedimentation effects, and solvent evaporation can be obtained (74). In this experiment, both stress and frequency remain at a fixed value within the linear viscoelastic regime.

2.2 Fluids

In order to fully comprehend the many exciting characteristics behind non-Newtonian fluids, in the context of shear, it is essential to establish what is a Newtonian behavior. Newton’s law of viscosity introduces a relationship between the fluid’s resistance to flow, and the stress applied.

Most materials do not uphold Newton’s law of viscosity, although some fluids commonly used in the day-to-day life are Newtonian. A few examples are water, air, oil, and honey. These materials, when analyzed at fixed pressure and temperature, have a constant shear viscosity (9).

When Newtonian fluids are introduced into simple shear flows, the only stress generated is the shear stress (34). Both normal stress differences, N_1 and N_2 are found to be zero (50). Newtonian fluids are modeled by the following constitutive equation:

$$\boldsymbol{\tau} = 2\mu\,\mathbf{D} \tag{2-1}$$

where D is the rate of deformation tensor defined as $\frac{1}{2}(\nabla V + \nabla V^T)$.

It was quickly observed that most materials shifted from Newtonian behavior. These, referred to as non-Newtonian fluids, exhibit compelling characteristics responsible for the deviations in the linear trend of the shear rate and viscosity curves.

Many examples of non-Newtonian fluids can be found in routine applications, ranging from everyday materials to complex formulations. Industries such as food, cosmetics, and oil either produce or work with these materials. Some of them are ketchup, hair gel, ink, cement, drilling fluids, and blood.

Non-Newtonian fluids can be separated then into distinct groups, according to the relationship between the rate of deformation and the stress tensor.One interesting behavior of non- Newtonian fluids is related to the viscosity, which can either decrease or increase under shear (34).

For many materials, the viscosity is found to decrease with the shear rate increases. This is known as a shear-thinning behavior (34). Viscosity can also increase with an increase in shear rate, giving rise to the shear-thickening behavior (51).

Some materials are ideally viscous liquids, while others may be ideally elastic solids. Between them are fluids that display viscoelastic behavior. When submitted to shear deformation, these fluids display a tendency to try to restore their initial state after a given time, in agreement with the Hookean deformation law.

Several materials that are shear thinning, also exhibit viscoplastic behavior. For a viscoplastic or yield stress material to flow, it must be submitted to a stress higher than the yield stress. Below the yield stress, these fluids display a solid-like behavior. The yield stress was introduced as the yield stress by Bingham in the 1920s (10). Colloidal suspensions, foams, gels, clays, greases, pastes, paints, and emulsions are examples found throughout almost all industries.

According to the dictionary, the verb "to yield" means "to give way to force or pressure". This definition gives a good qualitative description of many materials' behavior, implicating that these undergo an abrupt change to a much less resistant state beyond the yield stress (8).

Thixotropy is a behavior that can be characterized by its time-dependent structure and by the reversibility of the material's response to shearing. A non-Newtonian fluid can also display thixotropic behavior exhibited by its different responses to the same applied shear rates. Hence, if there is a gradual recovery of structure when the stress, previously applied to the material, is removed (34).

Although it is fair to say viscoplastic materials are characterized by yield stress, members of the scientific community have yet to come to a consensus for the concept of yield stress. According to Coussot et al. (19), viscoplastic materials flow homogeneously above the yield stress, and deform homogeneously below it.

The viscoelastic behavior of yield stress materials, both before and after yielding, has been recognized in many studies. A possible elastic nature of the yield stress is currently being discussed due to the presence of normal stresses (22, 72). Although, very few have tried to introduce this idea into the studies of constitutive equations for viscoplastic materials.

The rheological equations of state, also known as constitutive equations, illustrate the relationship between the stresses applied and the material's response to it, the deformation (51). These can be obtained while looking at a microstructural point of view or from analyzing the fluid as a homogeneous continuum (34).

Since the start of the last century, rheologists have created different equations that attempt to mimic the fluid's behavior. Although these models show a significant correlation to the fluid's mechanical behavior for most materials, it does not account for all of its mechanical phenomena. A generalized constitutive equation was created for non-Newtonian fluids:

$$\boldsymbol{\tau} = 2\eta(\dot{\gamma})\,\mathbf{D} \tag{2-2}$$

These were developed to characterize the relationship between shear rate and shear stress. For viscoplastic materials, the Herschel-Bulkley and the Bingham are the most popular models (30). Both models are presented in equations 2-3 and 2-4, respectively.

$$\begin{cases} \eta(\dot{\gamma}) = \dfrac{\tau_y}{\dot{\gamma}} + k\dot{\gamma}^{n-1}, & \text{if } \tau > \tau_y \\ \dot{\gamma} = 0, & \text{if } \tau < \tau_y \end{cases} \tag{2-3}$$

where τ_y is the yield stress [Pa].

This model results in highly complex numerical solutions. When n=1, the Bingham equation can be found.

$$\begin{cases} \eta(\dot{\gamma}) = \dfrac{\tau_y}{\dot{\gamma}} + \eta_p, & \text{if } \tau > \tau_y \\ \dot{\gamma} = 0, & \text{if } \tau < \tau_y \end{cases} \tag{2-4}$$

where η_p is the plastic viscosity [Pa.s].

These equations exploit the relationship between shear stress and shear rate, analyzing only one direction. It was assumed that the material was a Generalized Newtonian Fluid to extend this shear stress kinematic relation to a tensorial model.

These models will be referred to in this study as simple viscoplastic models (30) or as purely viscoplastic models (72).

As listed by Thompson et al. in (72), these models generally assume that (i) the material is always at equilibrium from the microstructure viewpoint; (ii) the material is inelastic; (iii) the material exhibits no normal stress differences in viscometric flows; and (iv) the von Mises yielding criterion applies. Consequently, according to these models, the yield stress is exclusively related to the shear stress at yielding.

This simplicity is the most attractive characteristic of the simple viscoplastic models, as pointed out by Frigaard et al. (30). These models do not consider the different roots of the yield stress, such as normal stresses, granular/jamming, polymeric, colloidal, or others.

Thompson et al. (72) argued that this analysis reduces the yield stress to a material property obtained through the simplest description of the viscoplastic phenomenon. This interpretation would lead to a generalization of the yield stress materials, assuming that the yield stress tensor would only have a shear component.

In the work published by Brader et al. (13), a dynamical yield criterion was proposed using a schematic single-mode coupling theory. The main idea was to introduce a complete prediction of the rheological behavior in nonergodic materials such as colloidal glasses. It was shown that the resulting yield stress approached that of the empirical form of the Von Mises criterion.

Ovarlez et al. (31) performed two original experiments to illustrate the possibility of a three-dimensional continuum description of the behavior of soft glassy materials. A three-dimensional jamming criterion was reported to be the plasticity criterion encountered in most solids. Among the other findings was that the fluids studied' viscosity was inversely proportional to the main shear rate. Also, these fluids behave as simple liquids in the direction orthogonal to that of the main flow.

Also published by Ovarlez (64) was a study of concentrated emulsions' rheological behavior. Interesting relations between the interstitial fluid and the suspensions studied were proposed and investigated. Both fluids presented the same index while being modeled by Herschell-Bulkley. Also, shear-induced migration with similar properties to Newtonian fluids was observed, suggesting that particle normal stresses could be proportional to shear stresses. Theory and experiments showed a nonzero normal stress difference at the yielding transition. Finally, a shear-dependent microstructure was indicated for these materials as the yield stress at flow start seemed to be different from that of flow stoppage.

2.3
Normal stresses

For a complete description of the behavior of an elastoviscoplastic fluid, it is important to characterize the full deviatoric stress state. The researches discussed in the following paragraphs studied normal stresses in viscoplastic materials, subject of interest in the present work.

So, the shear stress values, τ, the first and second normal stress difference N_1, and N_2 are necessary. These values are functions of the shear rate. If we denote "1" as the direction of the flow, and "2" as the direction of the shear gradient, then the normal stress differences can be defined as:

$$N_1 = \tau_{11} - \tau_{22} \tag{2-5}$$

$$N_1 = \tau_{22} - \tau_{33} \tag{2-6}$$

Stress is defined as the intensity of force, divided by the area in which the force is distributed. In solid mechanics, the greek symbol sigma (σ) represents normal stresses. A positive sign is used for tensile normal stresses, while a negative sign is used for compressive normal stresses, according to their convention (67).

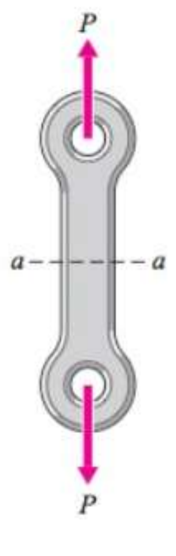

Figure 2.2: Loaded bar (67)

The example of a loaded bar, as shown in figure 2.2 is much used to study normal stresses in solid mechanics. In this simple experiment, axial forces are presented as forces normal to the exposed surface. The normal stresses are the intensity of the internal forces being transmitted while the material is under deformation (67).

In solid mechanics, normal stresses are used to explain basic problems such as the one presented in figure 2.2. At the same time, in fluid mechanics, simple flow systems are easily explained through the concept of shear stresses. In order to better comprehend more complex systems, it is essential to evolve from these basic paradigms. So, the simplicity in treatment used in solid mechanics cannot be given to the analysis of normal stresses for complex fluids.

When subjected to flow, materials can either remain unchanged, shrink (shear contraction) or expand (shear dilatancy) (40). Although this behavior is usually linked to solid materials, many complex fluids have also shown this nature.

When sheared, some non-Newtonian fluids present a force normal to the applied shear plane, called the normal force (21). Historically, normal stresses in shear flows were the first evidence of elasticity in liquids. Nowadays, since there are many easier ways to determine if the fluid is viscoelastic or not, normal stresses are being investigated for more exciting purposes and more critical applications.

The Weissenberg effect was the first documented evidence of the existence of normal forces in non-Newtonian fluids. It describes an experiment done for both Newtonian and non-Newtonian fluids in which a rod rotates steadily in a container. The Newtonian sample is pushed outwards by centrifugal forces (11), while for the non-Newtonian liquid, with measurable normal stresses, the sample climbs the rod, exhibiting the opposite behavior (12). This renowned effect can be seen in figure 2.3.

Figure 2.3: Rod climbing effect (11)

Since the first findings by Dr. K. Weissenberg, the scientific community has made great progress regarding normal stresses. In 1947, Weissenberg proposed that the second normal stress difference should be considered precisely zero in shear flows. Although the scientific community has shown that this theory is not correct, it still is a good first approximation for some problems (11). In 1967, Williams showed that at low shear rates, the first and second normal stress differences have the same sign for rubbery liquids and very dilute solutions. Some researchers have also suggested theoretical models that propose a relationship between shear stress and the first normal stress difference (6, 57).

Another finding was the Poynting effect, characterized by positive normal stresses when most elastic solids, including metals, rubbers, and polymer gels, dilate perpendicularly to the shear plane. This effect may happen when an elastic material is subjected to large shear strains, but the deformation is not enough to induce significant yielding or plastic flow (46).

In 1992, Ohl et al. (63) studied the second normal stress difference for pure and highly filled viscoelastic fluids. A pure polyisobutene and a 34.5% suspension of the same fluid were the materials investigated in this work. Experimental results showed that the values of the second normal stress difference were of the same magnitude or even larger than those of the first normal stress difference for the systems studied.

A study published by MacDonald et al. (49) in 1997 documented the rheological characterization of an ideal Boger fluid at shear rates close to the critical condition for an elastic instability. Cone-plate and parallel-plate geometries were used to map the desired behavior. Effects on the first normal stress difference were thoroughly analyzed. The authors reported a transient decrease in normal stress values under an applied shear steady state. The timescale for this unusual event was much larger than the polymer molecule's relaxation time. Various phenomena were investigated, and most of them discarded as the cause for this interesting effect on the first normal stress difference. Polymer migration was suggested to be associated with this unexpected behavior.

Acoutlabi et al. (5) performed an experimental study about different methodologies to measure both normal stress differences of viscoelastic liquids using an ARES rheometer. An original pressure sensor plate was introduced into the rotational rheometer to measure the pressure's radial profile. A standard poly(isobutylene) solution was used. The methods proposed in this work were through the pressure distribution of the cone-plate geometry (also known as PDCP) and the parallel-plate geometry (also known as PDPP) and through the total force cone-plate parallel-plate (TFCPPP). Good agreement between both normal stress differences and the certified results were reported for both pressure distribution methods. The N_1 results found were for the total force cone-plate parallel-plate method. Finally, in contrast with literature results, large positive N_2 values were found.

In more recent work done by Mao et al. (53), agar gels' solid-gel transition was addressed. In this study, a complete analysis of these types of gel's rheological behavior was done using parallel-plate geometry. A wide range of thermoreversible gels experiences a volume contraction during the sol-gel transition that is usually neglected. Normal forces were used to control the effects of this contraction. A zero normal force was applied to measure the linear properties of agar gels accurately.

An experimental approach to the relationship between shear stress and the first normal stress differences in shear thickening suspensions was introduced by Jomha et al. (40). They studied three concentrated suspensions, namely Superclay (supplied by English China Clays, Cornwall, U.K.) in water, polyvinylchloride in dioctylphthalate, and polystyrene latex in water, at volume concentrations of 40%, 48% and 60% respectively. The behavior of these materials' normal stress was analyzed against a polymer melt, polyethylene, and a polymer solution, composed of polyacrylamide in a 50/50 mixture of glycerol/water. The relationship observed was found to be similar when considering the different classes of materials studied in this work. Also, the authors reported this relationship between shear stress and the first normal stress differences to be independent of temperature. Finally, an abrupt behavior change was noted at the onset of shear thickening and beyond.

Baird (7) investigated the behavior of the first normal stress differences in polymer melts. A slit-die is used in the experimental setup to measure the hole pressure of the materials studied at high shear rates. Values of N_1 were obtained from calculations using the hole pressure, and compared to values measured using a cone-plate device. The experimental data presented in this work was in good agreement with the one measured using the cone-plate device, validating the experimental setup proposed.

A polystyrene melt was the material chosen by Schweizer (70) to perform an experimental study of the first and second normal stress differences. A cone and a partitioned plate tool were the instruments used in this work. Step shear rate tests were performed for different radii. A strong dependence of normal force response on cone angle was reported in this work. Reproducible and reliable data for first and second normal stress differences were presented and discussed in this study.

In 1979, Gadala Maria (32) first reported finding normal stress differences in sheared non-Brownian suspensions using measurements in a parallel plate rheometer. It was later reported by Kolli et al.(45) the dependence of the transient normal force signal and torque signal on the direction of the previous shear. When shear restarted in the opposite direction of the previous shear, normal force decreased, reaching a negative minimum and slowly gaining a positive steady-state value. On the other hand, it was reported that when shear was restarted in the same direction as the previous one, the normal force went rapidly from zero to its positive steady-state value.

Zarraga et al.(37) performed measurements regarding concentrated suspensions of non-colloidal spheres. This work studied N_1 and N_2 for a constant viscosity viscoelastic fluid. A rotating plate viscometer and profilometry of the suspension surface deflection near a rotation rod were the tools used to perform this paper's measurements. The results showed that the material displayed positive N_1 values, while N_2 was negative. The magnitude of N_1 was associated with the viscoelasticity of the suspending fluid. The value of N_2 at high concentrations was similar to other studies for suspensions in Newtonian fluids.

A study addressing the rheopetic effect in the flow of highly concentrated emulsions at low stresses through an experimental analysis is done by Massalova et al. (56). Normal stresses were investigated in this work. Measurements showed constant normal stress values at low shear stresses and an abrupt decrease in those values above the range of rheopetic behavior. In the low shear stress domain, the normal stress effect was associated with dilatational effects. The sharp decrease in normal stresses was said to be "apparent" and explained by rotational flow instabilities.

Wen et al. (76) published a study about the local and global deformations of filamentous biopolymers. Oscillatory amplitude sweep measurements were carried out, and the second normal stress difference was analyzed as a function of strain. Negative normal stresses were reported in the fibrin networks studied, as pointed out in this work. This behavior was also observed in other biological gels. Also, normal stresses seemed to increase as a function of strain and decline as the sample softens after rupture.

An experimental approach to measure normal stress differences and the particle phase distribution to the normal stresses in suspensions of non-Brownian hard spheres was proposed by Dbouk et al. (20). The radial profile of normal stresses along the velocity gradient direction in a torsional flow between two parallel discs was measured. N_1 and N_2 values were calculated from the slope, and the origin ordinate of the curve obtained from the measurements performed. The results obtained showed positive N_1 and negative N_2 signs.

An analysis of normal stresses for a suspension of neutrally buoyant non-Brownian spheres in a Newtonian viscous liquid was done by Garland et al. (33). In this work, measurements were performed using a cylindrical Taylor-Couette device of the shear-induced radial normal stress. Firstly, the slid pressure (P_g) and the membrane pressure (P_m) are measured in the experimental protocol. This measurement is then related to the fluid phase's radial normal stress and the radial component of the suspension's total stress, respectively. The results found were that for low shear rates, the subtraction of P_g-P_m was equal to the radial normal stress of the particle phase. The membrane pressure (P_m) was similar to the values of N_2 of the suspension stress.

Ahonguio et al. (4) present an experimental approach to the non-inertial flow of a yield stress fluid around spheres. The fluid showed elastoviscoplastic behavior when the bulk rheology was analyzed. A thorough analysis of the drag force was presented in this study. The drag coefficient was obtained through the hydrophobic properties and surface roughness. The total drag force was then separated into shear stress drag force and the drag force due to pressure forces and the first normal stress differences. The first was calculated by integrating the wall shear stress on the surface of the sphere. The second was obtained by subtracting the shear stress drag force from the total drag and was more significant than the first.

A theoretical approach to the relaxation dynamics of the normal stress of polymer gels is proposed by Yamamoto et al. (77). A two-fluid model was used to study these cases in which the gel is twisted by a rotational rheometer in a parallel plate geometry. The equations of motion of solvent and polymer network were obtained through the study of statistical thermodynamics. The theory presented in this work predicted positive normal stresses at the start of the experiment, followed by an exponential decay with time caused by the solvent's redistribution.

In Pan et al. (65), a study surrounding oscillatory and rotational rheology on shear-thickening granular suspensions was performed. The particle diameter and gap sizes between two parallel plates were systematically varied in this work, and its effects were analyzed. An interesting transition from positive to negative normal stresses was observed as a result. It is believed that the positive normal stresses arise from the frictional interactions, which determine the shear thickening behavior of suspensions. As for the negative normal stresses found, authors believe the increase of the particle diameter or decrease of gap size leads to a higher contribution of the hydrodynamic interactions.

With the advancements made over the last decades, it has become possible to get more accurate data using rheological instruments. In 1994, Laun (47) did several experiments on an RPS rheometer and a homemade normal force cell using a cone-and-plate geometry on a polymer dispersion. In this paper, the results show negative values of the first normal stress differences. Furthermore, he observed apparent first normal stress differences proportional to apparent shear stress in the regime of strong shear-thickening (47).

Traditionally, it was assumed that N_1 was null or positive for all shear rates. Kiss and Porter (44) analyzed concentrated solutions of Poly(-Benzyl-Glutamate) and observed negative values of N_1-N_2 at the intermediate shear rate values. The same N_1 sign variation behavior was verified for other fluids by Cato et al. (17), and Nakajima et al. (60).

Calado, White, and Muller (15) measured normal stresses for Boger fluids undergoing shear deformation. It was found that under prolonged shear in a cone-and-plate geometry, the normal stress curve for these fluids went from an initial plateau to the second plateau of lower values. This effect was explained by the conformational changes, possibly coupled to viscous heating of the sample responsible for decreasing the normal stress function. It is important to state that the materials exhibited positive first normal stress differences.

In work done by Labiausse et al. (46), aqueous foams, complex yield strain fluids, were studied. A nonlinear viscoelastic model for foam was presented, predicting a relationship between normal stress and shear stress oscillation amplitudes. The results obtained were compared to the Poynting relation, and even at strain amplitudes close to the yield strain, the approximation was good.

Kabla et al. (42) also investigated the behavior of an aqueous foam. The work studied the mechanical response of this viscoplastic material subjected to an oscillatory shear strain simulation. It was observed that the elastic domain was expanded when shear was progressively applied. This interesting behavior was associated with the appearance of an irreversible normal stress difference. Also, the effect of shear-induced plasticity on normal stress difference was thoroughly explored and presented in this work.

A second study completed by Kabla et al. (43) studied the aqueous foam's behavior both numerically and experimentally. Images of the sheared foam were taken to obtain the plastic flow profiles and the stress field's local statistical properties. The increase in the number of applied shear cycles resulted in continuous change in the normal stress differences measured in the aqueous foam.

A shaving foam, a hair gel, an emulsion paint, and a clay suspension were the materials used in work published by Shaukat et al. (2) in 2012. This study investigated the deformation behavior of thin films of these various soft glassy materials. The materials were submitted to two creep flow fields simultaneously, a rotational shear flow and an elongational flow. The elongational flow was responsible for some failures in the materials. The time to failure was found to be strongly dependent on the normal force as well as the shear stress. The Von Mises criterion was investigated and validated in this work.

Malkin and Masavola (52) were two of the first researchers to study normal stresses of highly concentrated emulsions undergoing shear deformation. In this work (52), flow curves show the shear rate dependence of normal stresses for high shear rates. At low shear rates, it was demonstrated that the dependence does not occur due to rheopexy. It is also stated that the transient stage is much longer for low shear rates than for high shear rates. Finally, the normal stresses exceed shear stresses for low shear rates.

In the work published by Verrelli et al. (75), the authors investigate the influence of the normal stress differences on the value of the yield stress and vice versa, for an elastoviscoplastic fluid. It was found that large normal stress differences may impact the behavior and characterization of yield stress materials. Firstly, if the shear stress is a function of the normal stress differences, it is important to know the full tensorial stress state at yielding. Secondly, the maximum shear stress in the material may be influenced by the walls' geometry, which might not be accounted for in the value of the normal stress differences.

Recently, Habibi et al. (35) obtained N_1-N_2 measurements for a commercial shaving foam and two different repulsive emulsions composed of 80% silicone oil in water. The measurements were performed using a smooth torsional parallel-plate geometry. Gap sizes were varied to better understand the effect of wall slip in the normal direction. Finite normal stress results were found after yielding. Negative normal stresses at low shear rates were associated with the surface curvature at the outer edge. Also, in this work, the curves were shifted so that they show a minimum of zero.

In 2016, Cagny et al. (23) found biopolymer gels exhibiting negative normal stress under shear. The findings showed a strange behavior since the normal stress response to an applied shear was positive for short periods but decreased to negative values with a characteristic time scale set by the pore size. It is also important to state that the magnitude of this negative N_1 was much larger than τ.

A study of normal stresses (N_1 and N_2) in a steady shear flow was proposed by Fazilati et al. (27). The work investigated the behavior of a Castor oil in water emulsion, two Carbopol® gels, and a shaving foam. Systematic steady shear rheological measurements were performed using both cone-plate and parallel-plate geometries with roughened surfaces. Values of N_1 and N_2 were compared. For the shaving foam and the Carbopol® gels, N_2 was negative and its value was lower than N_1. For the Castor oil in water emulsion, the value of N_2 was lower than N_1, but N_2 was positive.

In a more recent work done by Cagny et al.(21), authors point out that even though the Herschel-Bulkley equation has been used many times to describe a flow of a yield-stress material, it is far from a complete description of the material behavior. It is said that viscoplastic materials are known as elastoviscoplastic materials because of viscoelasticity both before and after yielding. Using a castor oil-in-water emulsion and two polymer microgel suspensions (Carpobol in water and a commercial hair gel), they measure two normal stress differences under continuous shearing and oscillatory flow. All systems showed positive N_1 values and negative N_2, both varying quadratically with the shear stress in both the unyielded and the yielded states. Finally, it was found that normal stresses do not go to zero when the shear rate does.

Viscoplastic materials tend to deform plastically. Therefore, it is essential to identify the yielding criteria for which the material will start to yield in a stress state. It is assumed that the Von Mises criterion is a condition of reaching a critical value of shear stress as the threshold of yielding (51).

The Von Mises criterion evaluates the energy that the material requires to change the form of a body; hence it is known as an energetic criterion. According to it, the yielding of the material will occur when the second invariant of the deviatoric stress tensor is greater than the yield stress value (28).

For a simple shear flow, with flow in the 1-direction, flow gradient in the 2-direction, and vorticity in the 3-direction, the Von Mises yield criterion can be written as:

$$N_1^2 + N_2^2 + (N_1 + N_2)^2 + 6\tau^2 = 2\sigma_y^2 \quad (35) \qquad (2\text{-}7)$$

where σ_y is the yield stress that would be measured in uniform uniaxial tension.

If no normal stresses are found, then τ_y should be equivalent to $\frac{\sigma_y}{\sqrt{3}}$.

In literature, the theoretical prediction's effectiveness using the Von Mises criterion has been thoroughly evaluated and validated (28, 31). Although, for viscoplastic materials, the normal stress contribution is usually neglected while using this criterion.

Recently, the discussion has arisen as to the effect of these stresses on the yielding criterion. Habibi et al. (35) found that the magnitudes of the normal stresses in shear contributed only a little to the relationship determined by the Von Mises criterion. Similarly, Cagny et al. (22) found that the normal stress contribution had a negligible effect (less than 1 %). These results go in agreement with the Von Mises criterion.

However, Thompson et al. (73) reported considerable normal stresses for similar materials. It was pointed out that these stresses dominated the yield surface caracterizations for these fluids. Also, Zhang et al. (78) suggested that the effect of normal stresses could result in finding a yield stress different from the value expected from the Von Mises criterion, reported in this work (78).

2.4 Summary

In this section, the concepts of rheology, rheometry, Newtonian fluids, non-Newtonian fluids, and viscoplasticity are addressed. A thorough analysis of the works about viscoplastic materials was done. Both Herschel-Bulkley and Bingham models were presented, and the simplicity of these models is discussed through works done by Thompson et al. (72), and Frigaard et al. (30). Classical studies published by Ovarlez et al. (31, 64) and Brader et al. (13) were also presented.

The review of normal stresses was divided into three parts. The first was a quick look into the definition of normal stresses from a solid mechanics perspective. A detailed analysis of the most relevant works in literature for normal stresses in fluids in general followed. The famous Weissenberg rod climbing effect and the poyinting effect were presented. Works that investigated normal stresses for viscoelastic fluids (63, 49, 5) were also discussed. Different methodologies for measuring normal stresses for polymer melts and their respective normal stress analysis (7, 70) were studied. Finally, the interesting results found on normal stresses for concentrated suspensions (40, 53) were thoroughly explored.

The last part of this section reported on the subject of interest in this work, normal stresses on viscoplastic materials, and the Von Mises criterion.

Kolli et al. (45) addressed how the previous direction of the shear affected both normal stress and torque signals. Positive N_1 values and negative N_2 values were found by for concentrated suspensions of non-colloidal spheres (37), suspensions of non-Brownian hard spheres (20), a shaving foam and two Carbopol® gels (27) and castor oil-in-water emulsion and two polymer microgel suspensions (21). In work published by Zarraga et al. (37), positive N_1 values were associated with the viscoelasticity of the suspending fluid.

Surprisingly, negative N_1-N_2 were reported by Kiss, and Porter (44). In work done by Habibi et al. (35), N_1-N_2 were measured, and for a commercial shaving foam and two different repulsive emulsions, negative normal stresses were found at low shear rates and associated with the surface curvature at the outer edge. Cagny et al. (23) presented negative normal stresses under shear for measurements performed for biopolymer gels. Similar results were obtained for a Castor oil-in-water emulsion in work done by Fazilati et al. (27).

Massalova et al. (56) pointed out the relationship between rheopetic behavior and normal stresses, observing constant normal stress values for low shear rates and a sharp decrease in the range of rheopetic behavior. In a study about filamentous biopolymers, Wen et al. (76) found that normal stresses increased as a function of strain in oscillatory amplitude sweep measurements. In work published by Pan et al. (65), measurements for shear-thickening granular suspensions presented an intriguing transition from positive to negative normal stresses. Calado, White, and Muller (15) found a normal stress curve with two plateaus, the latter with lower values, for Boger fluids.

Studies of different methodologies to obtain normal stresses were also presented in this section. Launn et al. (47) performed experiments using a homemade normal force cell with a cone-plate geometry on a polymer dispersion and found negative normal stresses. Dbouk et al. (20) measured the radial profile of normal stresses for flow between two parallel discs. Garland et al. (33) used pressure forces to calculate shear-induced radial normal stresses, while Ahonguio et al. (4) studied drag forces in work published.

Finally, the Von Mises criterion for viscoplastic materials was introduced. Works by Habibi et al. (35) and Cagny et al. (22) that found negligible contributions of the normal stress, validating the criterion analyzed, although studies by Thompson et al. (73) and Zhang et al. (78) suggested a discussion of this criterion due to discrepancies in their results.

As was presented in this chapter, there are huge discrepancies between the very few works that investigate the behavior of normal stresses on viscoplastic materials. The discussion has arisen in some research groups in the last years in an attempt to fill the gap in this field of study. The present work proposes an experimental approach to obtain and analyze normal stresses for yield stress materials.

3
Materials and Methods

3.1
Methodology

The materials' rheological properties were measured using a strain-controlled rheometer, namely TA Instruments' ARES-G2 (figure 3.1). It is equipped with an actuator for deformation control, a Torque Rebalance Transducer (TRT), and a Force Rebalance Transducer (FRT), guaranteeing independent shear stress and normal stress measurements. The transducer measures torques from $0.1\,\mu$N.m to 200 mN.m and normal forces from 0.001 to 20 N, respectively.

Figure 3.1: Rotational Rheometer: ARES-G2

All tests were performed at 25°C. A Peltier system was used to control the temperature of the material being tested. Also, a solvent trap with water was used in all tests to prevent evaporation, creating a saturated atmosphere around the sample.

The geometry was chosen according to the characteristics of the material tested. In this case, the desired rheological properties, namely normal stresses, were also taken into consideration. In order to obtain the forces imposed by the material, literature suggests the usage of plate geometries (35, 21).

The geometry selected had a 50 mm diameter, which was the largest available in the laboratory, aiming for larger sensitivity to normal stress measurements (21).

A parallel plate geometry allows for different gap sizes; the gap selected for these tests was 1 mm. For liquid dispersions, the gap must be expressively larger than the fluid tested's largest particle size (24).

Due to the yield stress, viscoplastic fluids present apparent wall slip at low shear rates (14), as usually observed in structured materials. A thin layer that does not slip but wets the wall and lubricates the flow is observed for these materials (35). This effect can lead to misinterpretation of the rheological measurements in the shear direction. Therefore, a rugged parallel plate was used in this work, as displayed in figure 3.2.

Figure 3.2: Rugged parallel plate geometries

However, it is believed in this work that the wall slip does not affect the normal direction results. The thin layer of liquid formed should not reduce or amplify the normal force imposed by the material; therefore, the value measured by the transducer should be that of the normal force of the material. Tests were performed to validate this theory and are shown in appendix A.

Flow in a cone and plate geometry with a small cone angle can be considered homogeneous and consequently ideal for a rheometric test. Because of the flow's homogeneity, a single shear rate can be associated with its shear stress. In a parallel-plate geometry, the flow is considered inhomogeneous in the radical direction. For a rotation velocity Ω, the apparent shear rate at a distance of r is $\Omega \cdot r/H$ (18).

Therefore, a technique that considers the shear rate heterogeneity and determines the effective constitutive equation in simple shear was proposed by Weissenberg-Rabinowitsch. The equation used for this correction is displayed in equation 3-1. TRIOS's software used in TA Instrument's rheometers offers this stress correction for parallel plate experiments in steady-state measurements.

$$\tau_R = \frac{2M}{\pi R^3}\left[\frac{3}{4} + \frac{1}{4}\frac{d\,ln(M)}{d\,ln(\dot{\gamma}_R)}\right] \tag{3-1}$$

Where, M is the torque, R is the plate radius and $\dot{\gamma}_R$ is the shear rate.

Before each test, the rheometer performs a conditioning transducer step, a conditioning sample step, and a pre-shear step. The conditioning sample is used to guarantee that the sample reaches the desired temperature before beginning the test. In the conditioning transducer step, the normal transducer force mode is switched to Spring Mode, as suggested by TA Instruments' instructors. The torque transducer force mode remains at FRT. The motor state was locked, and the torque and normal force were set to zero.

Firstly, air and oil were tested, then our viscoplastic materials. A syringe was used to place the oil in the rheometer. As for the viscoplastic materials, the sample is placed using a spatula or a glass syringe. The sample was always placed in the center of the geometry to ensure that it would spread homogenously. If bubbles are found after loading, they were removed by suction with a needle syringe.

Following the sample placement, the upper plate is lowered by 0.5 mm each time to minimize the residual stress tensor's effects once the test starts. Then, the upper plate is positioned slightly above the final gap position, and the sample excess is trimmed using a cotton swab. Finally, the geometry is brought to its final position, and the solvent trap is placed. This methodology is described in the diagram represented in figure 3.3. The material should be as displayed in figure 3.4.

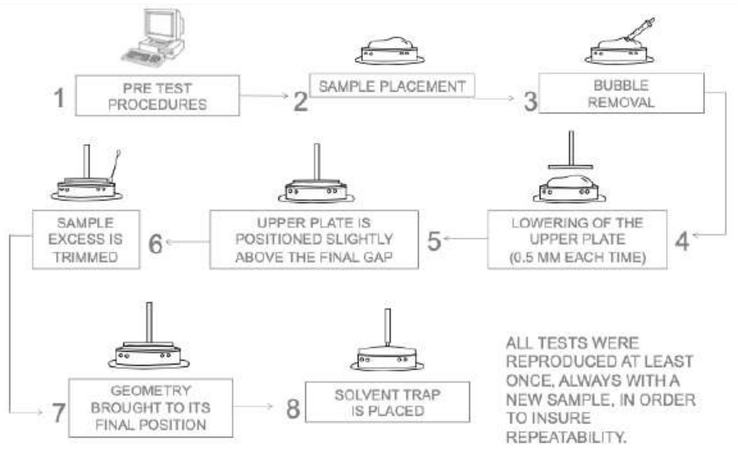

Figure 3.3: Representation of the sample placement procedure

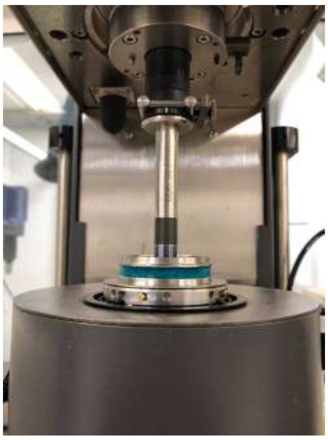

Figure 3.4: Sample placed on rheometer

All tests were reproduced at least once, always with a new sample, to ensure repeatability.

There are many challenges for measuring normal stresses in a shear deformation; some of them are temperature changes (15); sample loading and gap closing procedures that may lead to residual normal stresses (22); surface tension effects at geometry edges (7); and instrument inertia and alignment (21).

The flow curves were obtained and the viscosity function was fitted to the Herschel-Bulkley model, equation 2-3. This curve fit was done on the MatLab software, using the least-squares method.

3.2 Rheometrical experiments

The following rheometrical tests can be employed to obtain the rheological properties of interest that characterize the behavior of the materials studied:

- Flow curve

  In this test, viscosity is measured as the shear rate varies within a chosen range. Each point is measured when shear stress or viscosity has reached a steady state. For each data point, shear stress measurements are taken each 30 s and compared in groups of three. If the difference is smaller than 0.1%, the data point is taken. This procedure is repeated for a maximum of 1000 s for each data point.

  It is recommended that the measurements be from the higher shear rates to the lower ones to reduce each test's duration. When the material undergoes high shear rates, the sample is pre-sheared, and so the time needed to reach the steady-state is smaller.

  The viscosity function, given by the ratio of the shear stress and shear rate, was then obtained and fitted to the Herschell-Bulkley equation. Then, the rheological parameters, tau_y, k and n are determined. Also, normal stresses were analyzed against shear rate to characterize the fluid's behavior in the normal direction.

- Stress ramp

  In this test, stress is varied within a chosen range to determine the material's viscosity and deformation response. This test has the same objective as a flow curve, but it takes transient measurements.

  This test was used to perform transducer validation. The normal stress values were measured and plotted against the shear rate to analyze if the Newtonian fluids behave as expected in the normal direction.

- Peak Hold

  The material undergoes shear for a constant shear rate value for a selected time. Then, the behavior of stress is analyzed over time. As the stress reaches a constant value, the steady-state has been reached.

  In this experiment normal stress values were analyzed to see if they reached a steady-state. If so, the time needed to reach this steady-state in the normal direction was examined. Also, the values obtained in this test was compared to those measured in the flow curve for further discussion.

3.3 Materials

In this section, the materials used in this work will be presented. Newtonian fluids were used in equipment calibration and for the transducer validation. Stress ramps were done to analyze the fluid's behavior in the shear direction, for the equipment calibration, and in the normal direction, for the transducer validation.

Also, viscoplastic materials were studied for their interesting characteristics in the normal direction. A Carpobol® dispersion, two different hair gels, and a concentrated emulsion were analyzed. Flow curves and peak hold tests were performed for this characterization.

3.3.1 Newtonian Fluids

In this work, Newtonian fluids were used to perform the transducer validation and equipment calibration. Air and a standardized oil, IPT 89, were chosen as the Newtonian fluids for this study.

3.3.2 Yield stress materials

3.3.2.1 Bozzano Hair Gel (Prolonged action)

A commercial hair gel, "Gel Bozzano" (Prolonged action), which is a concentrated Carbopol dispersion, was studied in preliminary work. This material is considered a simple (non-thixotropic) yield stress fluid. The hair gel is displayed in figure 3.5. According to the manufacturer, the ingredients present in the material are: aqua, triethanolamine, carbomer, PVP, propylene glycol, parfum, PEG-40, hydrogenated castor oil, diazolidinyl urea, trasodium edta, benzophenone-4, panthenol, butyphenyl methylpropional, iodopropynyl butycarbamate, linalool, limonene, CL 42090, CL 60730.

Figure 3.5: Bozzano Hair Gel (Prolonged action)

In this work, flow curves and constant shear rate tests were done to determine the material's rheological behavior. The flow curve revealed a shear-thinning behavior of the gel and the existence of yield stress. The analysis of this flow curve was done after the Weissenberg-Rabinowtisch correction. The corrected curve and its Herschel-Bulkley fit are presented in figure 3.6. The value of the yield stress obtained was 67 Pa.

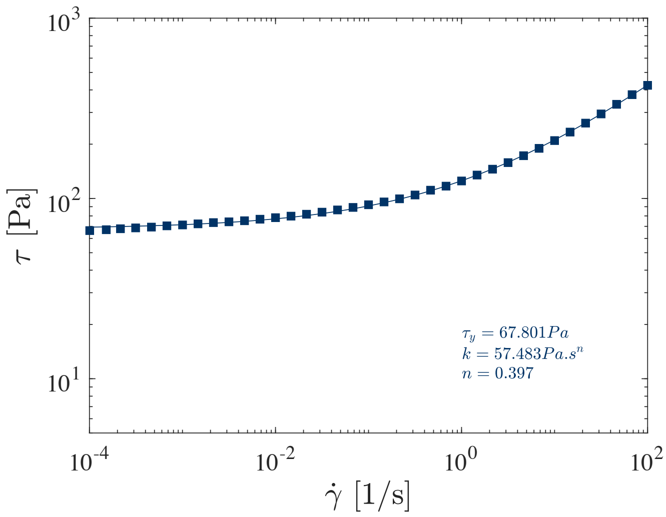

Figure 3.6: Flow curve: Bozzano hair gel (Prolonged action)

3.3.2.2
Carpobol dispersion

Carpobol® is a family of commercial polymers widely employed as a model fluid in research activities and used in industries such as pharmaceutical, paint, cosmetics, and food (16). Carpobol® polymers may be divided into different categories due to their physical structure and chemical composition (3).

It can be used as a rheological modifier as it is a dispersing, thickening, suspending, and stabilizing agent (74). Carpobol® dispersions indicate different rheological properties depending on the solvent used. In general, water is the solvent chosen. In this study, the Carpobol® aqueous dispersion were neutralized with a common base, sodium hydroxide (NaOH), which converts acidic polymer into a salt.

The dispersion of the Carpobol® polymer in the water at controlled pH and temperature forms a yield stress gel (19). The neutralized polymer can absorb and retain water. Irreversible agglomerates are formed after interconnected polymer chains begin to hydrate, increasing up to 1000 times their original volume, and partially uncoil (26). High molecular weight polyacrylate branched chains form entanglements that make it difficult for the fluid to flow at low shear stresses, causing the yield stress effect.

Carpobol® is generally considered a simple yield stress fluid (19). The rheological properties of this fluid are a function of temperature, concentration, pH, and fluid preparation (18). This material is usually well fitted by the Herschel-Bulkley equation (36), taking into account the yield stress and power-law shear-thinning behavior.

Carpobol® 940, used in this study, is a white powder, crosslinked polyacrylic acid polymer soluble in polar solvents. This polymer has a high molecular weight, and it is hydrophilic. The fluid preparation was done as described by Varges et al. (74).

In the present work, a Weissenberg-Rabinowtisch corrected flow curve and a Herchel-Bulkley fit was used to determine the material's yield stress, seen in figure 3.7. Shear-thinning behavior and the presence of yield stress were observed for this aqueous dispersion, as expected. The value of the yield stress found was 10 Pa.

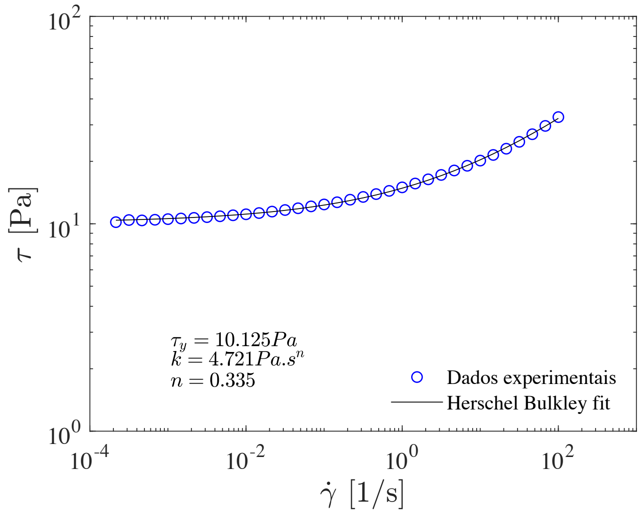

Figure 3.7: Flow curve: 0.1 % Carpobol 940 aqueous dispersion

3.3.2.3
Highly concentrated emulsion

A highly concentrated emulsion was prepared using a Crude oil as the continuous phase and a synthetic water as the dispersed phase. The synthetic water was made according to the ASTM Standard D1141-98.2013, "Standard Practice for the Preparation of Substitute Ocean Water" (71). Both the oil phase and synthetic water had their density measured at 40°C (temperature in which the emulsion was prepared), and the value obtained was 0.87 g/cm^3 and 1.01 g/cm^3, respectively.

Light crude oils may have a high viscosity at temperatures below their melting point with the formation of colloidal structures from waxy components. The complex nature and constant volatility of these components ask for a thermal pretreatment to allow better repeatability of the rheological results (54). The pretreatment temperature should be higher than the wax appearance temperature of the oil. In this work, the temperature used in this step was 60°C.

This work was done using a 70 vol% water in oil emulsion. To prepare this emulsion, firstly, 48.8 g of synthetic water was weighed in a glass bottle, followed by 24.3 g of Crude oil. After that, the glass was put in a bain-marie, previously heated at 40°C and homogenized using a magnetic stirrer at 150 rpm. A thermocouple was also used to control the system's temperature at 40°C for about 40 minutes before beginning the emulsification process. A dispersor ULTRA-TURRAX® T25 from IKA was employed in this process. During the first 10 minutes of the emulsification process, the rotation was 12000 rpm, followed by 5 minutes in a 14000 rpm rotation.

A quick study of the material's rheological behavior was primarily done through flow curves. This curve was corrected using the Weissenberg-Rabinowitsch method. The highly concentration emulsion showed, as the other materials presented in this work, a shear-thinning behavior. The yield stress found was 4 Pa. Figure 3.8 illustrates the corrected curve and the Herschel-Bulkley fit used to obtain the yield stress.

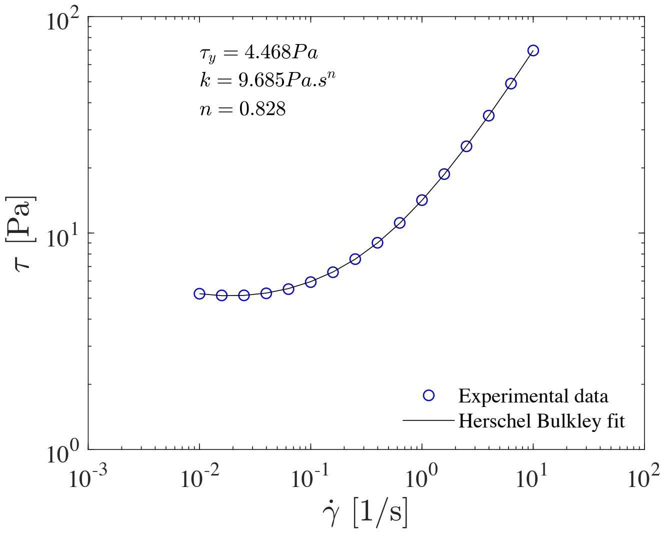

Figure 3.8: Flow curve: Highly concentrated emulsion

3.3.2.4 Bozzano Hair Gel (Solar protection)

A commercial hair gel, "Gel Bozzano (Solar protection)" shown in figure 3.9, was chosen to be studied in this work. This material is also considered a simple (non-thixotropic) yield stress fluid. According to the manufacturer, the ingredients present in the material are: aqua, triethanolamine, carbomer, PVP, propylene glycol, parfum, PEG-40, hydrogenated castor oil, diazolidinyl urea, trasodium edta, benzophenone-4, butyphenyl methylpropional, iodopropynyl butycarbamate, linalool, limonene, CL 19140.

Figure 3.9: Bozzano Hair Gel (Solar protection)

Flow curves and constant shear rate experiments were performed to obtain this second hair gel's rheological characterization. The flow curve obtained was corrected by the Weissenberg-Rabinowtisch equation. The material presented a shear-thinning behavior, with the existence of yield stress. Both the corrected flow curve and its Herschel-Bulkley fit can be found in 3.10. The value of the yield stress obtained for the "Gel Bozzano (Solar protection)" was 48 Pa.

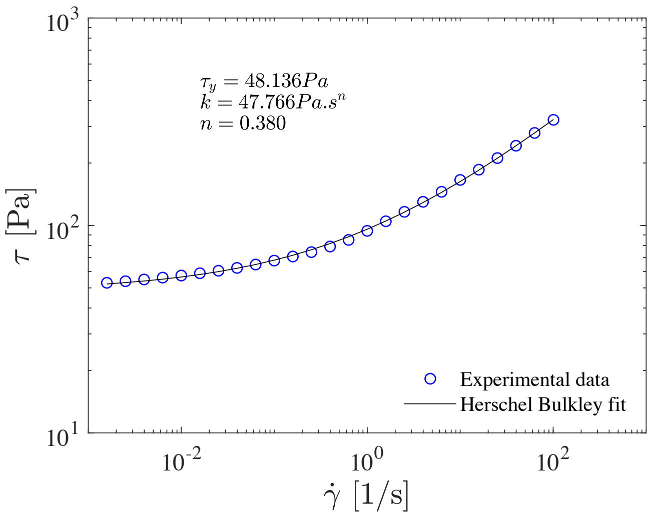

Figure 3.10: Flow curve: Bozzano hair gel (Prolonged action)

3.4 Transducer Validation

The ARES-G2 is equiped with a force rebalance transducer (FRT) in which the rotational position of the core remains fixed while eletromagnetic forces are used to counteract the applied normal force. The electromagnetic current flowing leads to the magnitude of the measured normal forces. Due to the sensitivity of this equipment, studies were conducted to analyze the compliance of different force rebalance transducers (62, 69).

In this study, air and oil were used to do flow ramp tests in order to validate the transducer used. The flow ramps ran from 100 Pa to $1x10^{-4}$ Pa. These are both Newtonian fluids, and as expected, the normal force remained constant and equal to zero. Figures 3.11 and 3.12 represent the plots of normal forces against shear rate for both air and oil, respectively. The tests validated the transducer measurements.

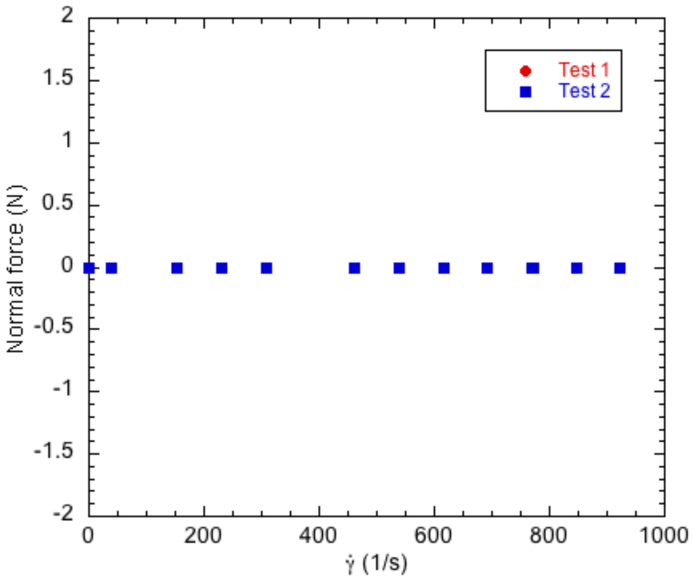

Figure 3.11: Normal force x Shear rate for air

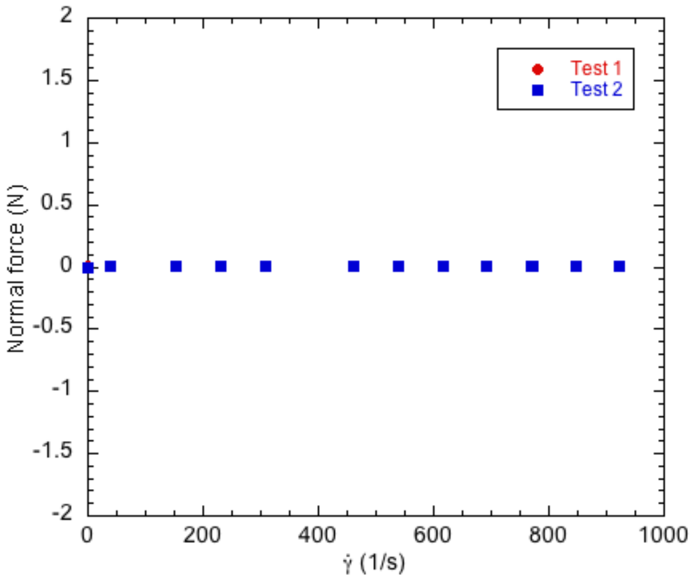

Figure 3.12: Normal force x Shear rate for oil

4
Results and Discussion

The tests performed in this work included flow curves and constant shear rate. These were explained in Section 2.1. These tests were chosen to study the behavior of the normal stresses differences undergoing shear deformation for both transient and steady-state measurements. The flow curves were performed for values of shear rate from 100 s^{-1} to 1x10^{-3} s^{-1}, or values in between. These data were obtained under rate control. For shear rates varying from the values mentioned before, constant shear rate tests were executed. The measurements in this section were done using a cross-hatched parallel plate geometry with the exception of the preliminary results. The analysis and discussion of the results obtained are described in this section.

4.1
Preliminary results

Preliminary work performed with commercial hair gel Bozanno (prolonged action), described in section 3.3.2.1, are presented in this first part of the results. Flow curves and creep tests were made to investigate normal force measurements for elastoviscoplastic materials. These measurements were done using a parallel plate smooth geometry.

Firstly, flow curve results will be presented. Flow curves were performed for shear rate values varying from 50 s^{-1} to 0.0001 s^{-1}.

Figure 4.1 shows normal force plotted against shear rate. High values of normal force are obtained at the beginning of the test. After that, as shear rate decreases, the normal force curve decreases until it reaches a plateau. The second curve plotted (Test 2) starts to decrease again after 0.001 s^{-1} and the normal force values reach negative values at the end of the test, which is not seen in the first curve (Test 1). Both curves show a Herschell-Bulkley behavior when normal force is plotted as a function of the shear rate.

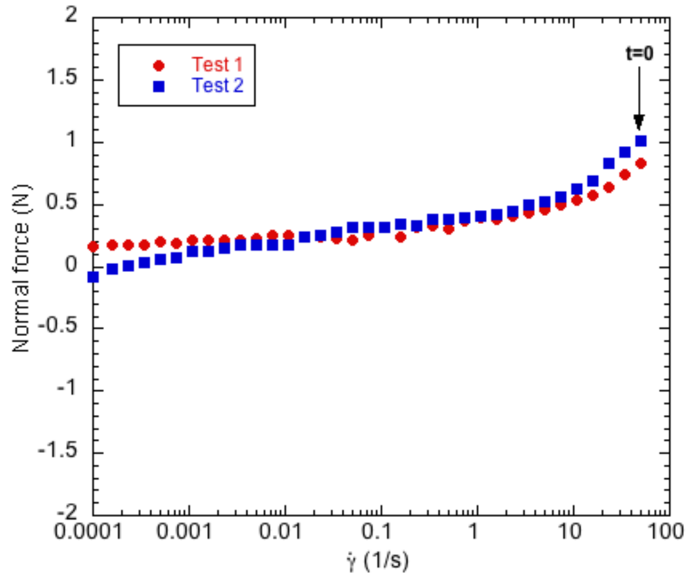

Figure 4.1: Bozanno hair gel (prolonged action): normal force x shear rate

Figure 4.2 shows the normal force as a function of the step time. At the beginning of the test, for high shear rates, high normal force values are obtained. As shear rate decreases, normal forces lower and reach a plateau. For the second curve, Test 2, the normal force curve decreases again for even lower values. This discrepancy between tests is expected, seeing as the long duration of these tests may cause effects such as fluid evaporation.

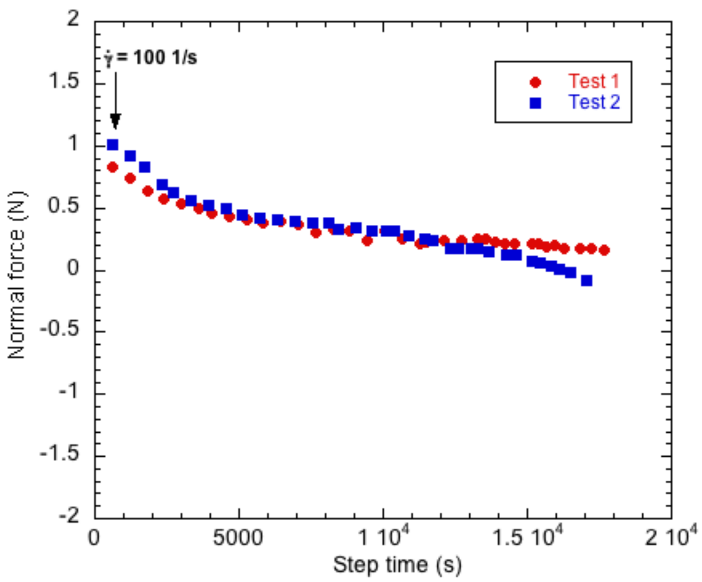

Figure 4.2: Bozanno hair gel (prolonged action): normal force x step time

.

In figure 4.3 both shear stress and the normal stress difference are plotted against shear rate for both curves, Test 1 and Test 2. In this graph, shear stresses are represented by closed symbols, while $N_1 - N_2$ values are represented by open symbols. Both shear stress and normal stress differences curves have similar Herschell-Bulkley behavior. It is seen that for higher shear rates, the values found for $N_1 - N_2$ are much higher than those found for shear stresses. Interestingly, for lower shear rates, both normal and shear stresses appear to have similar values. It is important to point out that for this graph, rugged geometry was used to avoid wall slip.

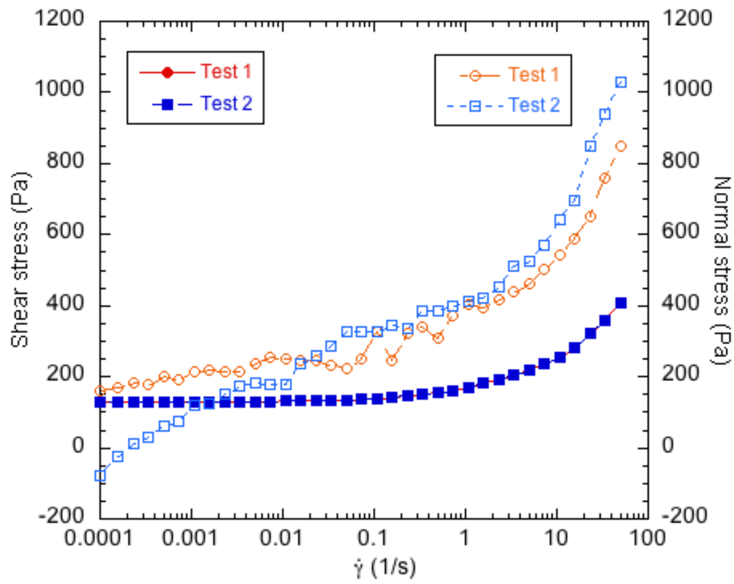

Figure 4.3: Bozanno hair gel (prolonged action): shear stress and normal stress against shear rate

Creep tests were performed for stresses lower than the yield stress. Firstly, constant shear stress of 1 Pa was imposed, followed by 30 Pa.

Figure 4.4 shows the normal force curve plotted against time for the creep test done for shear stress of 1 Pa. The material appears to have reached the steady-state for the normal force curve after about 1000 s. After reaching steady-state, both curves reach a plateau for the normal force value of -0.4 N. Thus, a long transient period is expected for normal direction measurements.

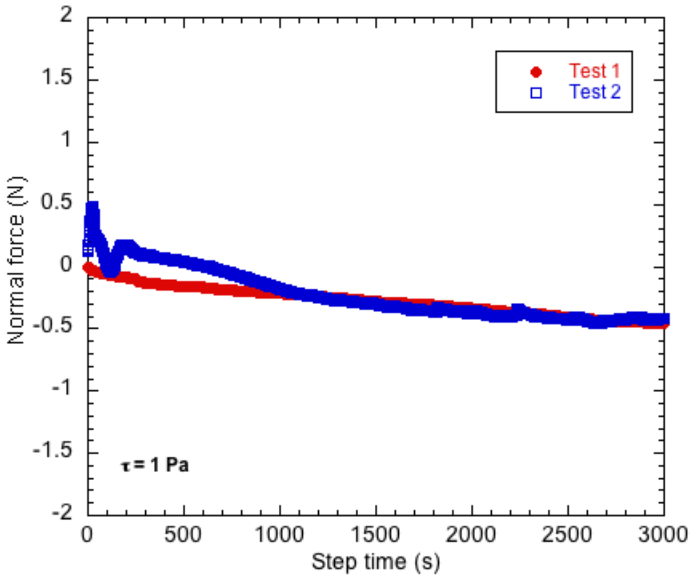

Figure 4.4: Bozanno hair gel (prolonged action): normal force x step time

Normal force was plotted against the step time in figure 4.5 for shear stress of 30 Pa. It takes about 100 seconds for the material to reach the quasi-steady state for the normal force curve. After reaching a quasi steady-state, both curves reach a plateau for the normal force value of -0.2 N.

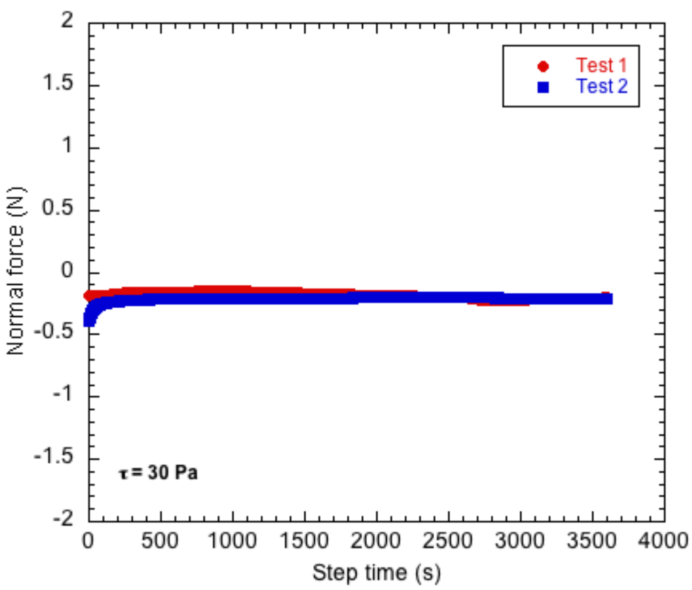

Figure 4.5: Bozanno hair gel (prolonged action): normal force x step time

This round of preliminary results were key to develop and set an experimental protocol for the three materials studied in this work. This stimulating discussion lead to many interesting findings presented throughout the rest of this chapter.

4.2 Carbopol

For the first part of this analysis, different plots and variables were studied from results obtained in a repetitive flow curve test. This flow curve was performed for values of shear rate from 100 s^{-1} to 1x10^{-3} s^{-1}.

Firstly, the consistency of the data studied in this section is checked through the analysis of the normal force *versus* torque plot. This is shown in figure 4.6. The rheometer used is equipped with a force rebalance transducer (FRT), which apparently shows no anomalies in the results discussed in this section. The curve illustrates that results were obtained for high torque values, which are applicable in the equipments' sensitivity, and show consistent and reliable data.

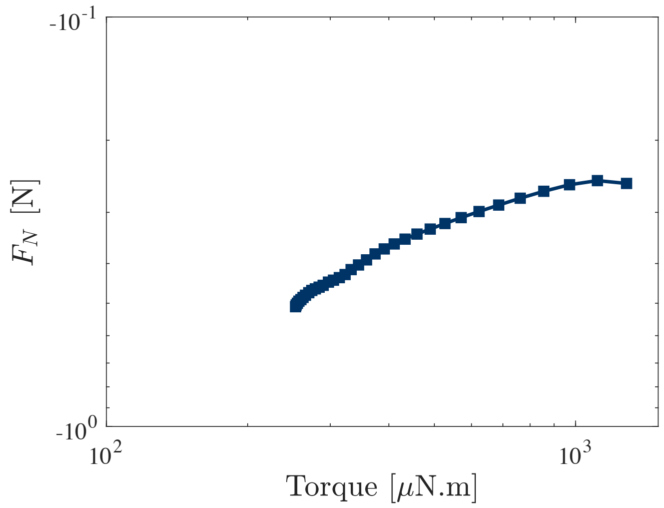

Figure 4.6: Carbopol: normal force *versus* torque

Normal stress differences *versus* shear rate plots were constructed from the results found in the corrected flow curve, as can be seen in figure 4.7. It is important to mention that, for each data point in this test, the steady-state is measured in terms of viscosity and shear stress and not normal stresses. The equipment software takes a data point when viscosity and shear stress remains unchanged with time.

No positive $N_1 - N_2$ values were found for this material in this type of test. Three slopes can be seen in the curve in figure 4.7. The first would be a linear one with the first three points, followed by a second slope until 0.1 s when the curve changes its inclination again. For higher shear rates, the values of N_1 are somewhat smaller in magnitude than those found for lower shear rates. Also, when shear rate values approach the equivalent value of the yield stress, the slope of the curve changes, illustrating the impact of the yielding process.

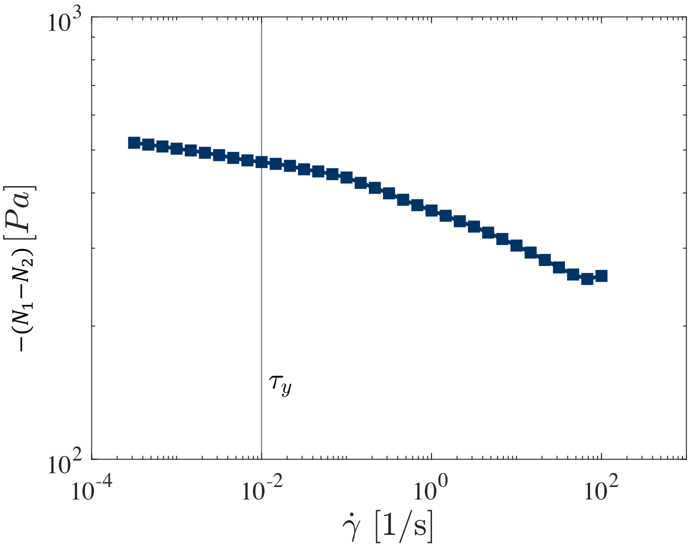

Figure 4.7: Carbopol: normal stress differences *versus* shear rate

Figure 4.8 illustrates $N_1 - N_2$ values as a function of shear stress using the corrected flow curves results obtained in the ARES-G2 rheometer. A similar behavior as seen in figure 4.7 was observed. For values above the yield stress (10 Pa), two different slopes can be seen, a linear relation of normal stress differences against shear stress above 15 Pa and another just until the yield stress. Magnitude values of $N_1 - N_2$ found in this experiment reach as high as 500 Pa, again illustrating the importance of this ill-explored variable.

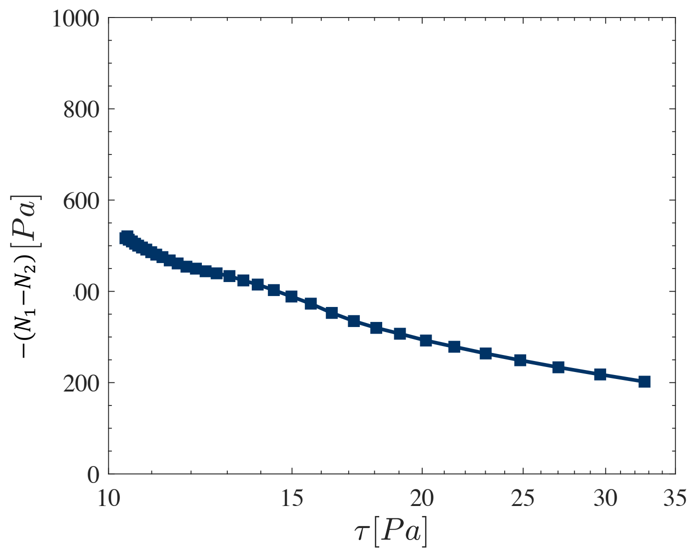

Figure 4.8: Carbopol: normal stress differences *versus* shear stress

The results illustrated in figure 4.9 form the core of this work. Data presents steady values of the shear stress and the absolute values of the normal stress differences. This plot exhibits the complexity surrounding the behavior of yield stress materials under flow deformation. Throughout the whole experiment, absolute values of $N_1 - N_2$ are higher than those of shear stress. On a smaller scale, this effect was also seen by Malkin et al. (52). This behavior contradicts the general idea that normal stresses are second-order effects.

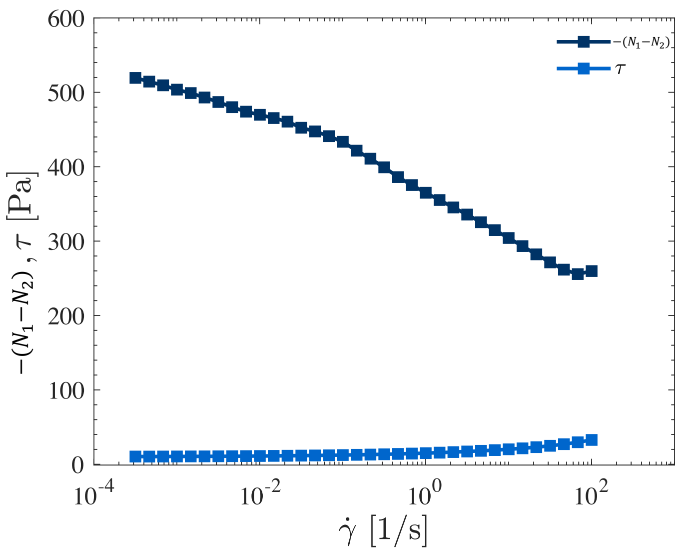

Figure 4.9: Carbopol: stresses *versus* shear rate

Figure 4.10 challenges the original concept of a Herschell-Bulkley fit. The shear rate dependence of $N_1 - N_2$ seen in the data presented in this section looks unexpected. In this plot, $N_1 - N_2$ values are submitted to fit the well-known Herschell-Bulkley equation as shown in figure 4.10. Some studies mentioned in this work (22, 72) raise the prospect of the existence of a "yield normal stress". The plot shows a well-fitted curve, illustrating that the normal stress reaches a finite value of parameter $\tau_{N,y}$.

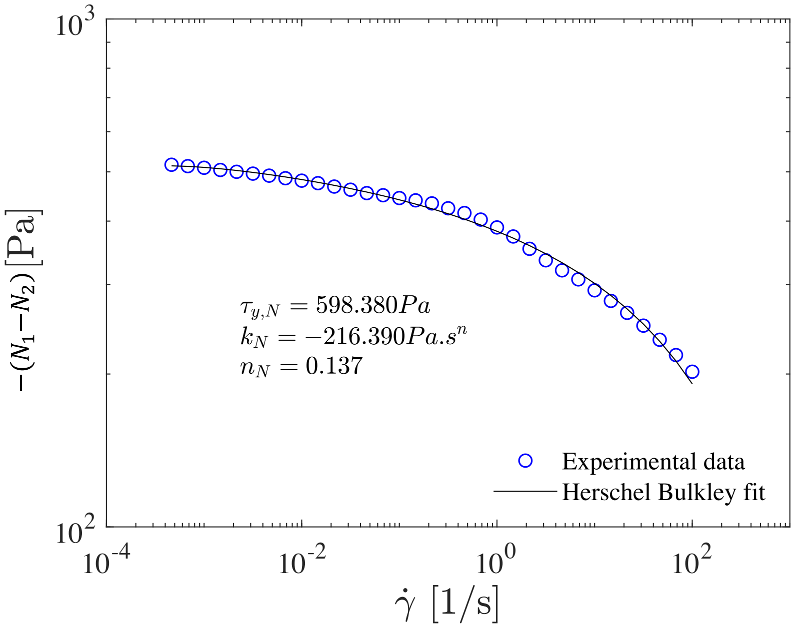

Figure 4.10: Carbopol: curve fit $N_1 - N_2$

Negative $N_1 - N_2$ values were normalized by the shear stress and plotted against shear rate in figure 4.11. The absolute values of the normal stress differences grow larger concerning the shear stress as the shear rate decreases. Therefore, the ratio between the two values is higher as the material gets close to the yielding region.

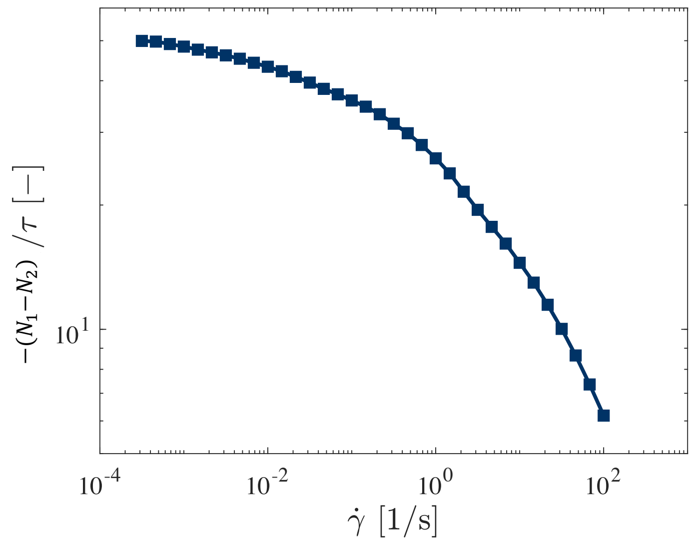

Figure 4.11: Carbopol: normalized normal stress differences *versus* shear rate

Figure 4.12 exhibits the behavior of the absolute values of the normal stress coefficient against the shear rate in the test studied. Absolute values of $\psi_1 - \psi_2$ are plotted against shear rate. ψ_1 values are calculated through $\psi_1 = N_1/\dot{\gamma}^2$. It was found that under prolonged shear, $\psi_1 - \psi_2$ values increases largely. Interestingly, due to the negative $N_1 - N_2$, the behavior of this curve is actually the opposite of most results found in literature (34). When plotted the negative values of the normal stress coefficient, as in figure 4.12, the behavior of the curve is the same found in literature.

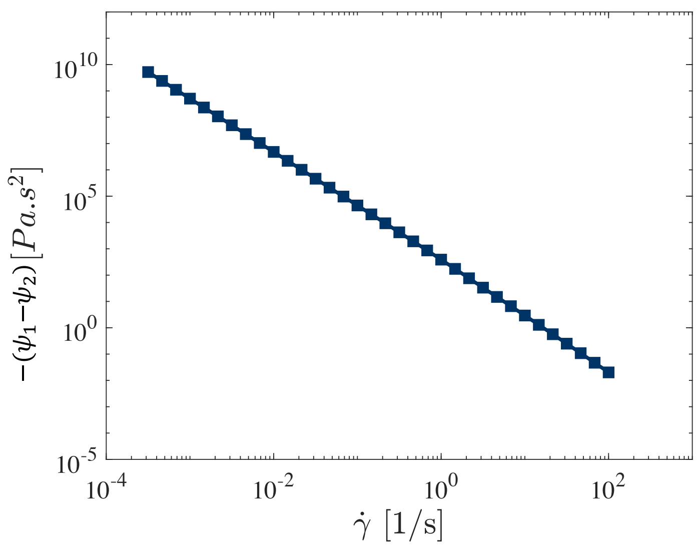

Figure 4.12: Carbopol: normal stress coefficient *versus* shear rate

Normal stress differences and viscosity are plotted against shear stress in figure 4.13. Data shows that the magnitude of $N_1 - N_2$ increases for lower shear stress, and consequently, higher viscosity. The shear-thinning behavior of this material's viscosity curves displays an inflection when the normal stress curve does, exhibiting very large values of both viscosity and normal stress differences.

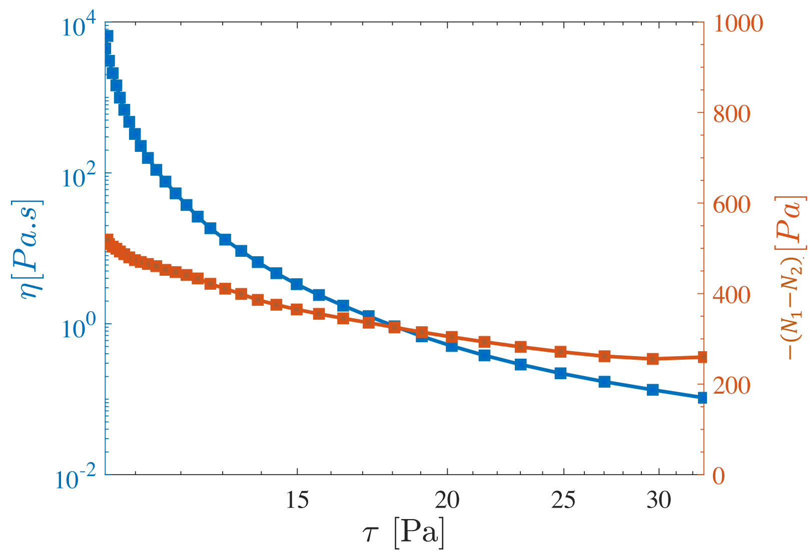

Figure 4.13: Carbopol: normal stress differences and viscosity *versus* shear stress

The following graphs illustrate the analysis done for constant shear rate experiments. The values of shear rate chosen for this study were 100 s^{-1}, 10 s^{-1}, 1 s^{-1}, 0.1 s^{-1}, 0.01 s^{-1}, and finally 0.001 s^{-1}.

$N_1 - N_2$ was plotted against shear rate, in figure 4.14. Dynamic data values were taken from the flow curve experiment, discussed in the first part of this section, and static data values were taken from the constant shear rate tests. The values chosen for the normal stress differences in the constant shear rate experiment correspond to those measured in steady-state for each of the shear rates studied in this part of the section. The error plot consists of three experiments of each of test.

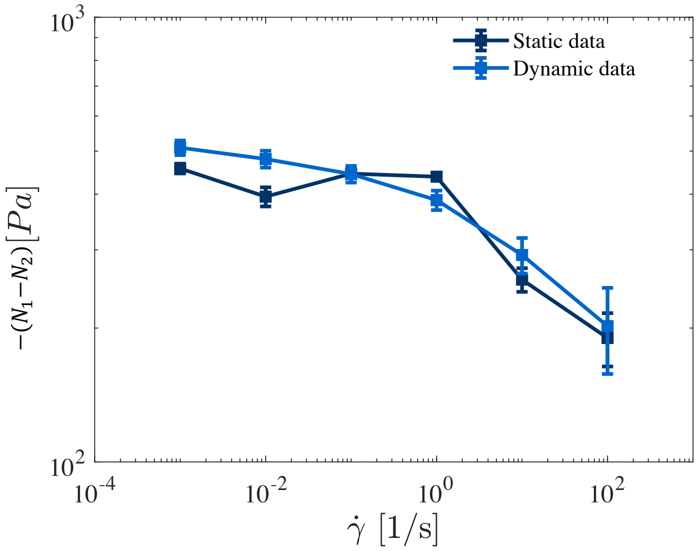

Figure 4.14: Carbopol: normal stress differences *versus* shear rate for constant shear rate tests and a flow curve test

Interestingly, values of N_1 vary little between the curves presented. The highest difference lies in shear rate 0.01 s^{-1}, about 18%. However, this difference is probably because the nonhomogeneous correction does not correct the constant shear rate experiments. This plot exposes the satisfactory results obtained in the flow curve experiments and discussed during the previous part of this section.

Another intriguing observation is that the biggest error bars are found for the highest shear rates. A simple but impactful explanation is proposed in this chapter. The interfacial tension may influence the values of $N_1 - N_2$ in rheometric experiments. The illustration displayed in figure 4.15 shows the relationship between the two stresses seen at the edge of the sample placed in the rheometer. The interfacial stress has an angle of contact in the air-liquid interface, but this will not be considered in this analysis due to the complexity of obtaining this contact angle. Thus it remains as a suggestion for future works.

Figure 4.15: Sample in the rheometer: interfacial and normal force analysis

In work done by Jörgensen et al. (41), surface tension measurements in Carbopol gels were performed. The yield stress and elasticity of the gel were taken under consideration. The estimation of surface tension was set at around 63 mN m^{-1}. The influence of rheology and protocols in surface tension measurements was highlighted in this study.

This impact was analyzed by calculating the interfacial force of the fluid in the rheometer and the normal force at the highest shear rate (100 s^{-1}) for the three constant shear rate tests (a,b and c) and are shown in equations 4-1 and 4-2.

$$F_{\sigma_s} = \frac{63}{1000} 2\pi \frac{D}{2} = \frac{63}{1000} 2\pi \frac{0.05}{2} = 0.01\,N \tag{4-1}$$

$$F_N = N_1 A = N_1 \frac{\pi D^2}{4} \tag{4-2}$$

$F_{N_a} = 0.37\,N$
$F_{N_b} = 0.47\,N$
$F_{N_c} = 0.40\,N$

The difference between the values found for F_{N_a},F_{N_b} and F_{N_c} varies from 0.03 N to 0.1 N, which is about one magnitude higher as the force caused by the interfacial effect, $F_{\sigma_s} = 0.01\,N$. The comparison between the two forces analyzed illustrates an influence of 33% to 10% on the significant error bars seen in figure 4.14. The uncertainty and standard deviation are higher than the absolute value of σ_s.

For each result obtained with all the different constant shear rate experiments, a curve of stress *versus* time was plotted. All curves were assembled in figure 4.16. For high shear rate values, it can be seen that stress values remain unchanging in time, which means a steady state is obtained quickly in the first seconds of the test. It is important to mention that these results have not been submitted to the nonhomogeneous correction as the flow curve results. That is why the values of shear stress differ from those obtained in the flow curve experiments.

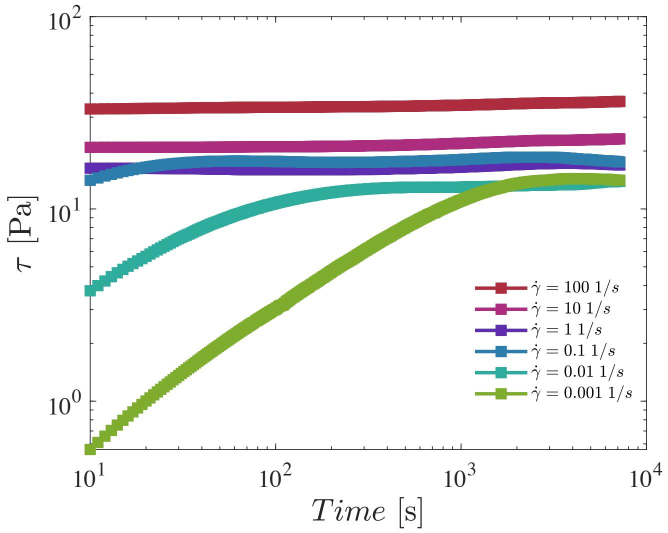

Figure 4.16: Carbopol: stress *versus* time

As the shear rate decreases, the time it takes for the stress to arrive at a constant value plateau grows longer. For the last shear rate chosen value, 0.001 s^{-1}, it takes longer than the maximum time waited for each data point in our flow curve experiment (10^3 s). In flow curve experiments, the material is being sheared throughout the whole test, arriving at a steady state sooner. The material's yield stress can be seen in the plateau obtained after 1000 s for both the 0.01 s^{-1} and 0.001 s^{-1} curves.

Figure 4.17 was constructed to analyze the comparison between two constant shear rate experiments. The values of shear rate chosen were 100 s^{-1}, high shear rate, with the shear stress higher than the yield stress of the material, plotted at the beginning of flow curve experiments and, 0.001 s^{-1}, which has shear stress equivalent to yield stress of the material, the lowest value of shear rate studied. Firstly, it is important to mention that, as seen in this graph, the time it takes for the $N_1 - N_2$ values to arrive at an unchanging value in time is extremely higher than that of the shear stress. That can be described for both experiments. Also, data shows values of normal stress differences much higher in magnitude than those of shear stress, as was analyzed in the flow curve tests presented in the first part of this section.

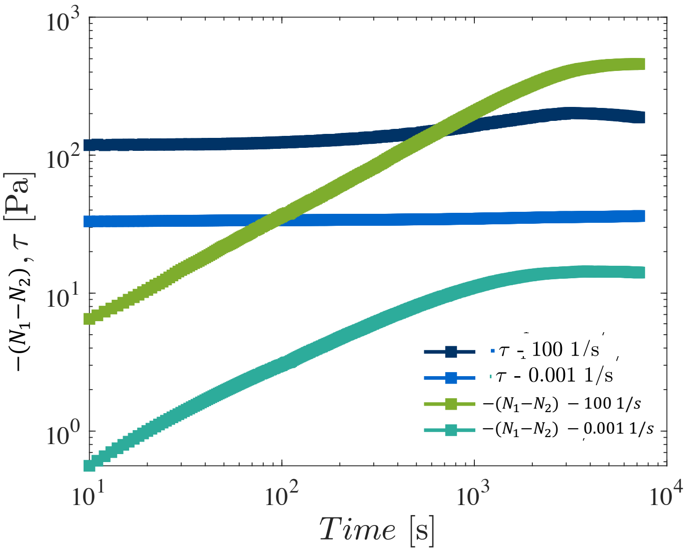

Figure 4.17: Carbopol: stresses *versus* time

The behavior of the normal stress differences in constant shear rate tests was analyzed over time in figure 4.18. The curves presented are for values of shear rate of 100 s^{-1}, 10 s^{-1}, 1 s^{-1}, 0.1 s^{-1}, 0.01 s^{-1}, and 0.001 s^{-1}. As seen for the shear stress graph presented in figure 4.16, as the shear rate increases, the time it takes for the steady-state to arrive in the normal direction decreases.

Also, the $N_1 - N_2$ value at the beginning of the test augments in magnitude as the shear rate increases, except for the 0.001 s^{-1} curve. This difference in trend could be explained by the initial condition of the sample, which is not necessarily the same. It is possible to have small structural variations of the material after sample placement. Therefore, the transient experiments are affected by the initial condition, whereas the steady-state tests are not.

However, the opposite result is obtained at the end of the test, constant values of $N_1 - N_2$ at a steady-state decrease in magnitude as the shear rate increases. Another interesting observation is that, for shear rate tests from 1 s^{-1} and lower, the value of normal stress differences obtained in the steady-state is practically the same. These $N_1 - N_2$ curves fall into the same plateau at about 5x10^{-3} s. This can be associated with a possible existence of a "normal yield stress".

The steady-state regime for curves displayed in figure 4.18 is obtained after the maximum time waited for each data point in our flow curve experiment (10^3 s). From this perspective, it is expected that the flow curve results for $N_1 - N_2$ differ from those obtained here. Although, as seen in figure 4.14, results are quite close. This behavior can be explained because the material is primarily submitted to a pre-shear in the flow curve experiments and is constantly submitted to shear, allowing the fluid to arrive sooner at the steady-state. The difference, however, can be attributed to the nonhomogeneous correction applied to the flow curve results.

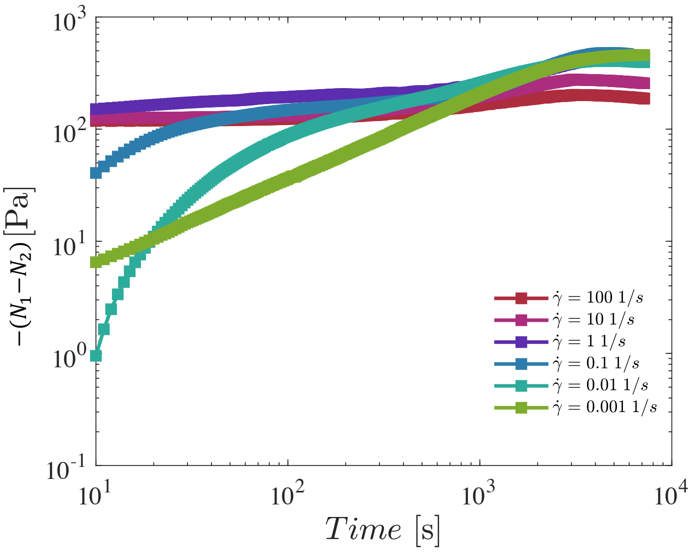

Figure 4.18: Carbopol: normal stress differences *versus* time

Figure 4.19 illustrates the first normal stress coefficient's behavior over time. For high shear rate values, $\psi_1 - \psi_2$ values are presented as a horizontal line in the log-log plot. For lower shear rate values, the same horizontal line is obtained on the steady state. Thus, absolute values of normal stress coefficient increase as the shear rate values decrease.

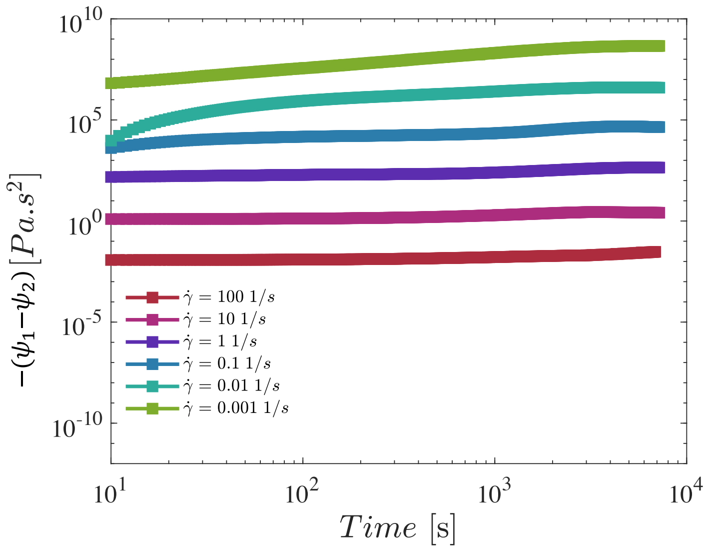

Figure 4.19: Carbopol: normal stress coefficient *versus* time

Normal stresses are very sensitive to microstructural changes that occur when the material is submitted to shear flow (29). Theory suggests that gels, such as the Carpobol gel studied in this section, are soft and deformable and therefore behave as a polymer, displaying finite normal stresses (22, 47). Also, a quick look into the material's storage G' and loss G'' modulus is presented in figure 4.20, and the elastic nature prior to yielding is clear.

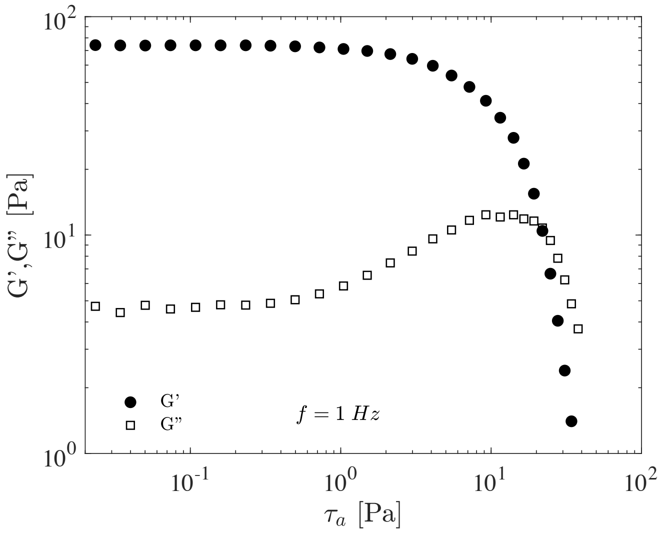

Figure 4.20: Carbopol: storage G' and loss G'' modulus with oscillatory test

4.3
Highly concentrated emulsion

Results obtained for a highly concentrated emulsion in a repetitive flow curve, performed for values of shear rate varying from 10 s^{-1} to 1x10^{-2} s^{-1}, will be studied in the first part of this section. Various plots and interesting variables will be discussed in a shorter analysis than found in section 4.2.

Steady state values of the shear stress and the absolute values of the first normal stress differences, found in figure 4.21, will be presented for the first discussion. As considered in section 4.2, in the flow curve experiments, steady-state measurements are taken in terms of viscosity and stress, not normal stress. Only negative values of $N_1 - N_2$ were found for the highly concentrated emulsion in this type of test.

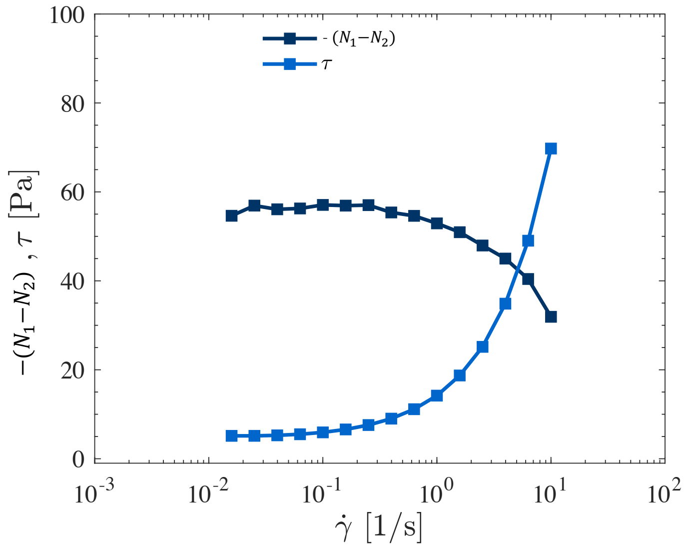

Figure 4.21: Highly concentrated emulsion: stresses *versus* shear rate

The plot in figure 4.21 illustrates, once again, the curious results surrounding normal stresses in yield stress materials. For most of the test, absolute $N_1 - N_2$ values are higher than shear stress. However, contrasting from results obtained for Carpobol gel and discussed in section 4.2, both curves "cross". Therefore, for high shear rates, absolute $N_1 - N_2$ values are lower than shear stress values. Interestingly, the behavior of the curves is quite similar but mirrored; while absolute $N_1 - N_2$ values augment when shear rate decreases, the opposite is found for shear stresses.

The experimental data was submitted to a Herschell-Bulkley fit in figure 4.22. As seen for the Carpobol dispersion in section 4.2, an interesting shear rate dependence of normal stress differences is found for the highly concentrated emulsion studied. The well-fitted curve presents a finite value of the parameter $\tau_{N,y}$. This parameter can be associated with the "yield normal stress" suggested in studies done by Cagny et al. (22) and Thompson et al. (72). Not surprisingly, as seen for the Carpobol dispersion, the value of this parameter is extremely higher than that found for the yield stress of this material ($\tau_y = 4.46\,Pa$).

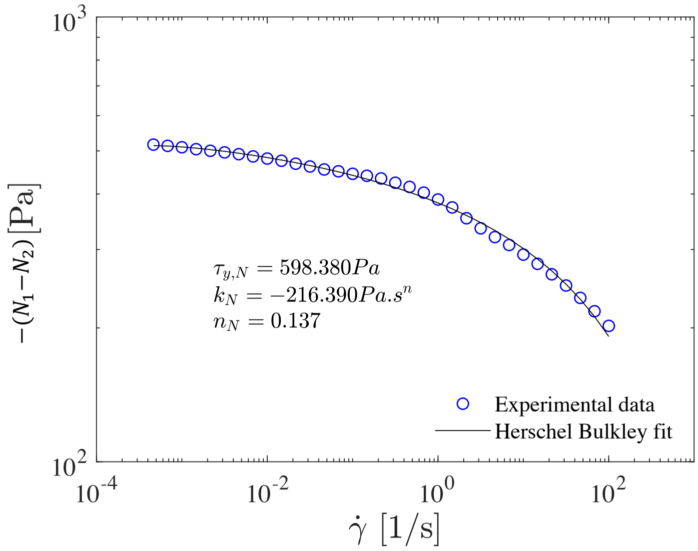

Figure 4.22: Highly concentrated emulsion: curve fit normal stress differences

In figure 4.23, a graph was plotted of the absolute values of $N_1 - N_2$ normalized by the shear stress of the highly concentrated emulsion against shear rate. As shear rate decreases, the ratio studied increases towards a plateau obtained when the material reaches the yielding region. A plateau in the domain of low shear rates was also clearly observed for highly concentrated emulsion in work done by Malkin et al. (52).

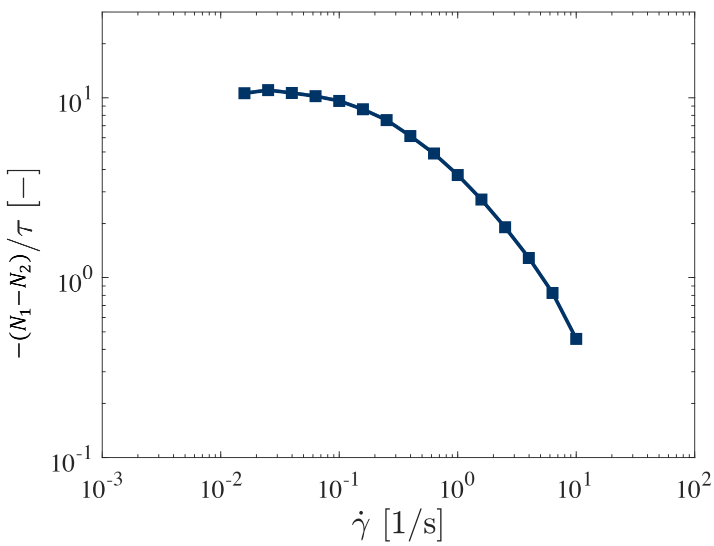

Figure 4.23: Highly concentrated emulsion: normalized normal stress differences *versus* shear rate

Absolute values of the normal stress coefficient are plotted against shear rate in figure 4.24. As shear rate decreases, the $-\psi_1$ values increase significantly.

Analogous to what was seen for the Carpobol dispersion in section 4.2, the behavior of the curve seen in 4.24 is similar to that found in the book by Barnes (34) due to the negative normal stress differences obtained for both materials.

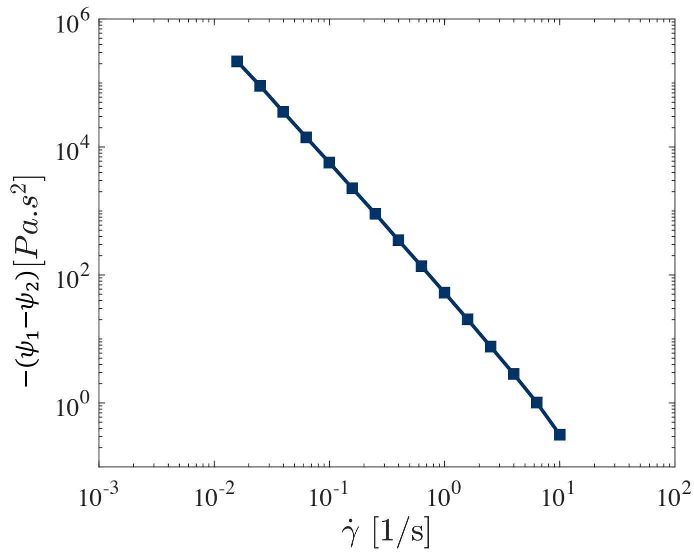

Figure 4.24: Highly concentrated emulsion: normal stress coefficient *versus* shear rate

For the second part of the highly concentrated emulsion analysis, constant shear rate experiments were studied. The values of shear rate chosen for this analysis were 10 s^{-1}, 1 s^{-1}, 0.1 s^{-1}, 0.01 s^{-1}, and finally 0.001 s^{-1}.

Firstly, dynamic and static data were chosen to construct the first graph, found in figure 4.25. Dynamic data was taken from the flow curve experiment, presented at the beginning of this section, and static data values were taken from the constant shear rate tests. For this comparison, absolute $N_1 - N_2$ values were plotted against shear rate. The error plot was constructed from three experiments of each type of test. Also, the values chosen for the $N_1 - N_2$ in the constant shear rate experiment correspond to those measured at the end of each test, which approximated to steady-state.

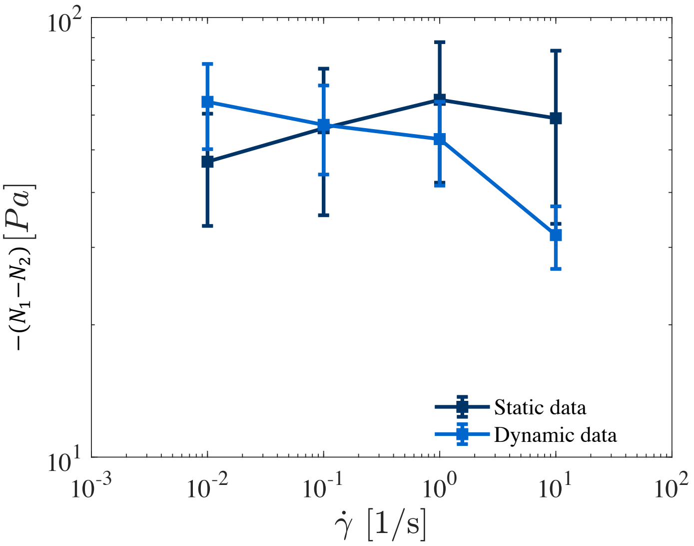

Figure 4.25: Highly concentrated emulsion: normal stress differences *versus* shear rate for constant shear rate tests and a flow curve test

Divergent to what was seen for the Carpobol dispersion in section 4.2, figure 4.25 presents unmatching results when comparing both constant shear rate and flow curve experiments. As mentioned before, in flow curve experiments, steady-state is measured for viscosity and stress, not normal stress. Also, the following graphs illustrate that the steady-state regime only appears to have been reached at the end of the constant shear rate experiments. It is important to mention that the nonhomogeneous correction is not applied to the constant shear rate experiments. The value found for 0.1 s^{-1} is similar in both tests, but it is probably a coincidence.

Habibi et al. (35) illustrate the importance of pre shear in tests involving foams and emulsions under continuous shear flow. This procedure would remove the residual normal forces that appear during sample placement. However, in the constant shear rate experiments found in figure 4.25, no pre-shear procedure was performed, while for the flow curve experiments, this procedure was carried out before the beginning of the test, as described in section 3.1.

According to Fazilati et al. (27), for emulsions and foams, normal stresses are attributed to the alignment of drops in flow direction and drop deformation. Also, in the work done by Habibi et al. (35), the effect of surface curvature and interfacial tension at the outer edge of plate-plate geometries is depicted. These effects could be deeply affected by sample placement and therefore have a stronger influence in transient experiments such as the constant shear rate experiments illustrated in figure 4.25.

Figure 4.26 illustrates the results obtained with the constant shear rate experiments. For this analysis, a curve of stress *versus* time was plotted for shear rate values of $10\,s^{-1}$, $1\,s^{-1}$, $0.1\,s^{-1}$, $0.01\,s^{-1}$, and $0.01\,s^{-1}$. It is critical to mention that these plots have not been submitted to the nonhomogeneous correction as the flow curve results. As a consequence, the shear stress values seen in figure 4.26 differ from those obtained in the flow curve experiments in the first part of this section.

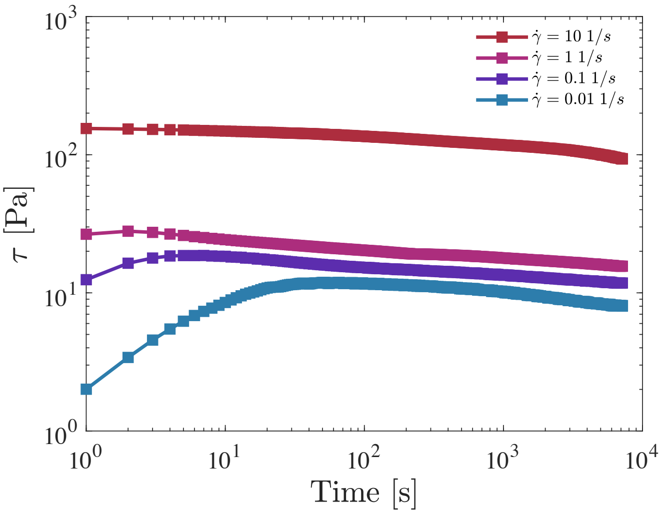

Figure 4.26: Highly concentrated emulsion: stress *versus* time

Similar to what was reported in the previous section (4.2), the steady-state was quickly obtained for the high shear rates. However, for lower shear rates, the time it takes to arrive at the steady-state grows significantly larger as the value of shear rate decreases.

The absolute values of $N_1 - N_2$ obtained in the constant shear rate experiments were plotted against time in figure 4.27. Constant shear rates experiments of $10\,s^{-1}$, $1\,s^{-1}$, $0.1\,s^{-1}$, $0.01\,s^{-1}$, and $0.01\,s^{-1}$ were chosen for this analysis.

In comparison with figure 4.26, steady-state values are obtained in much shorter times for shear stresses than the normal stress differences. That can be associated with all constant shear rate experiments studied. In addition, absolute $N_1 - N_2$ values are significantly higher than those found for shear stress. At the beginning of this section, this contribution was also seen in the discussion surrounding flow curve experiments for highly concentrated emulsions.

In contrast with the results previously discussed, positive $N_1 - N_2$ values were obtained at the beginning of the constant shear rate experiments. This difference in the normal stress' sign was also reported by Fazilati et al. (27) between Carbopol and highly concentrated emulsion results. As the material is submitted to shear, the material displays negative $N_1 - N_2$ values. This difference could be associated with the initial condition of the sample, which is not necessarily always the same. Small structural variations of the material can be seen after the sample is placed in the rheometer, leading to possible residual normal stresses. Consequently, constant shear rate tests would be more affected by the initial condition when compared to flow curve experiments. In work done by Habibi et al. (35), authors emphasize the implementation of a pre-shear procedure at the start of each experiment involving emulsions and foams under continuous shear flow to reduce the discrepancy at the beginning of the test.

When analyzing the normal stress differences' steady-state through the constant shear rate experiments found in figure 4.27, a log-log graph was constructed. A plateau-like structure can be seen at the end of the test and is better illustrated in figure 4.28. This horizontal line appears about two hours after the beginning of the test, which could affect the sample with problems such as evaporation and sedimentation. These issues may have influenced the difference between the static and dynamic data curves in figure 4.25.

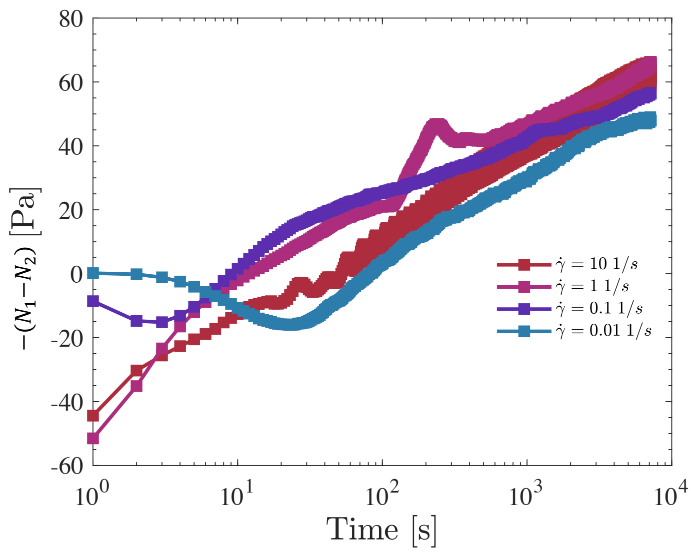

Figure 4.27: Highly concentrated emulsion: normal stress differences *versus* time (linear plot)

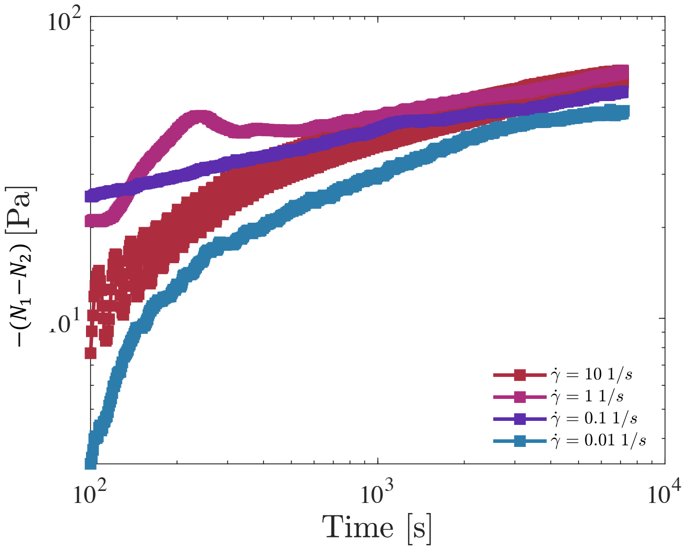

Figure 4.28: Highly concentrated emulsion: normal stress differences *versus* time (log plot)

The first normal stress coefficient's behavior over time was plotted in figure 4.29. $\psi_1 - \psi_2$ increases significantly in magnitude as the shear rate decreases, analogous to what was seen for the Carpobol dispersion in figure 4.19 in section 4.2 and the flow curve analyzed at the beginning of this section. After a transient period, for all shear rate values, a plateau illustrates the behavior of the normal stress coefficient in the log-log plot.

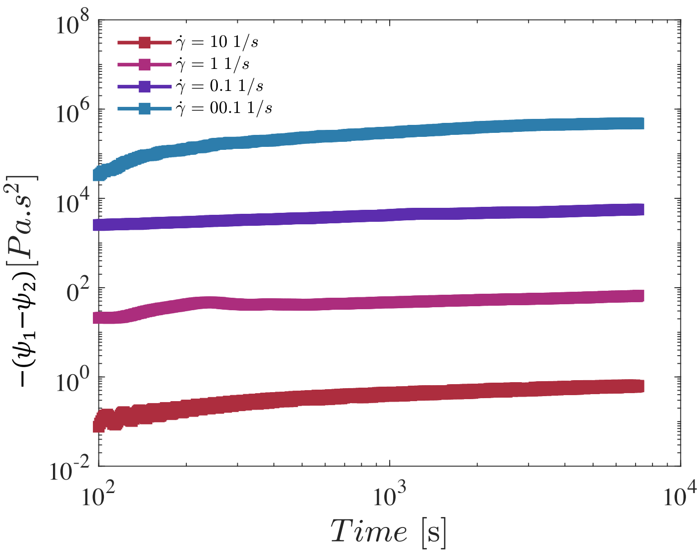

Figure 4.29: Highly concentrated emulsion: normal stress coefficient *versus* time

4.4
Bozzano Hair Gel (Solar protection)

Analogous to what was done in section 4.3, a smaller study than found in section 4.2 was performed for the Bozzano Hair Gel (Solar protection). Analysis surrounding key plots and variables will be presented in this section.

At the beginning of this section, flow curve results for the Bozzano Hair Gel (Solar protection) are presented. The flow curve was performed for values of shear rate going from 100 s^{-1} to 1x10^{-3} s^{-1}.

Figure 4.30 was chosen for the first discussion of this section. Absolute values of $N_1 - N_2$ and values of shear stress are plotted against shear rate. As mentioned in earlier sections, for the flow curve results, steady-state measurements are taken in terms of viscosity and stress, not normal stress. Similar to what was seen for the Carpobol dispersion and the highly concentrated emulsions, flow curve experiments resulted in negative $N_1 - N_2$ values throughout the whole test.

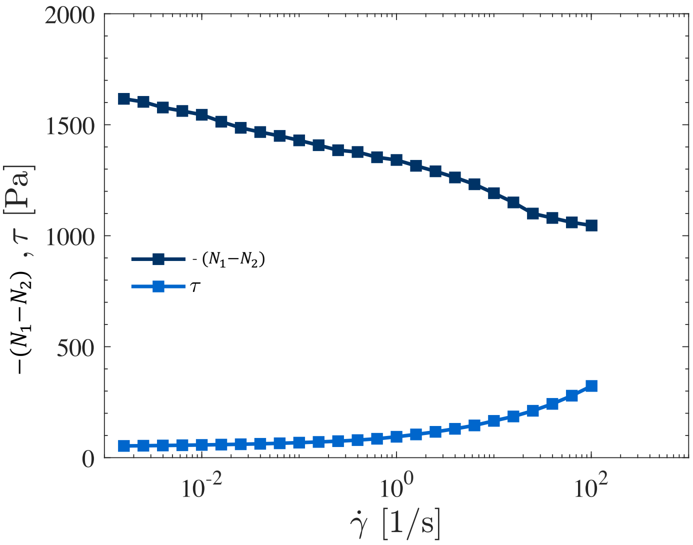

Figure 4.30: Bozzano hair gel (Solar protection): stresses *versus* shear rate

Interesting results for normal stresses in yield stress materials are exhibited in figure 4.30. Similar to what was found for Carpobol gel and contrasting to what was discussed for the highly concentrated emulsion, the absolute $N_1 - N_2$ values obtained are extremely higher than those found for shear stresses. In more intriguing results, from 100 s^{-1} to about 1x10^{-2} s^{-1}, and akin to what was seen for the highly concentrated emulsion, both curves present similar behavior but mirrored. Shear stresses decrease as shear rate increases, while absolute $N_1 - N_2$ values grow larger when shear rate decreases.

Unlike results presented in both sections 4.2 and 4.3, data obtained in the hair gel's normal stress flow curve could not be submitted to fit the Herschell-

Bulkley equation. As seen in figure 4.31 and compared to previous results, the shear rate dependence of normal stress differences looks rather abnormal. Three different behaviors can be seen in this plot. A horizontal line composes the first three points. Two linear slopes of different inclinations follow this curve.

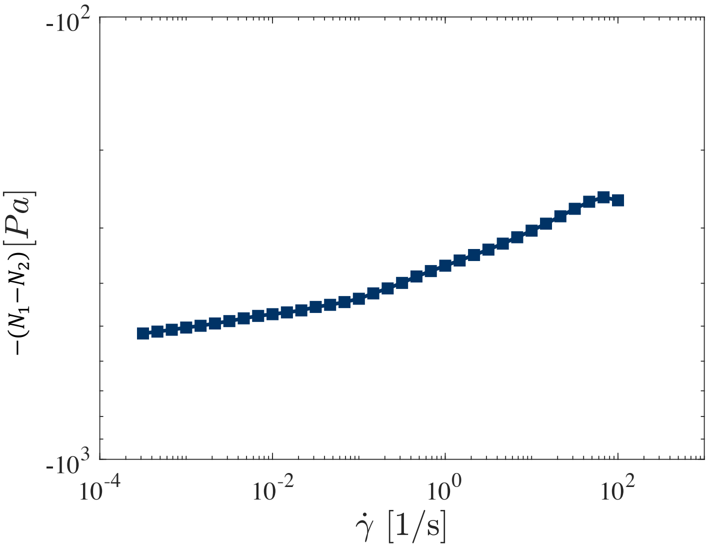

Figure 4.31: Bozzano hair gel (Solar protection): normal stress differences *versus* shear rate

Absolute values of $N_1 - N_2$ normalized by the shear stress of the commercial hair gel were plotted against shear rate in figure 4.32. The ratio between the two values increases towards a plateau as the material gets close to the yielding region; similar results were seen for the highly concentrated emulsion. However, after this, the ratio continues to increase as shear rate decreases.

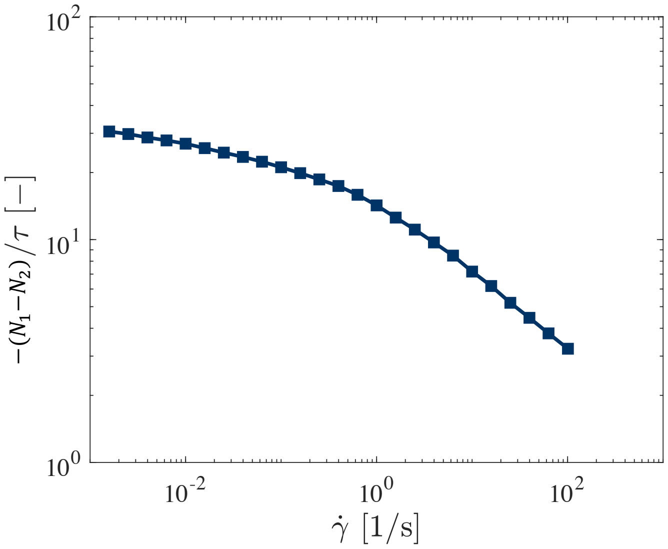

Figure 4.32: Bozzano hair gel (Solar protection): normalized normal stress differences *versus* shear rate

In figure 4.33, the behavior of the normal stress coefficient is illustrated. Comparable to what was seen for both the Carpobol dispersion and the highly concentrated emulsion, $-\psi_1$ values increase considerably as shear rate decreases. Also, due to the negative $N_1 - N_2$ values seen in the results of the three materials investigated in this work, the behavior of the curve found in figure 4.33 is analogous to those found in literature (34).

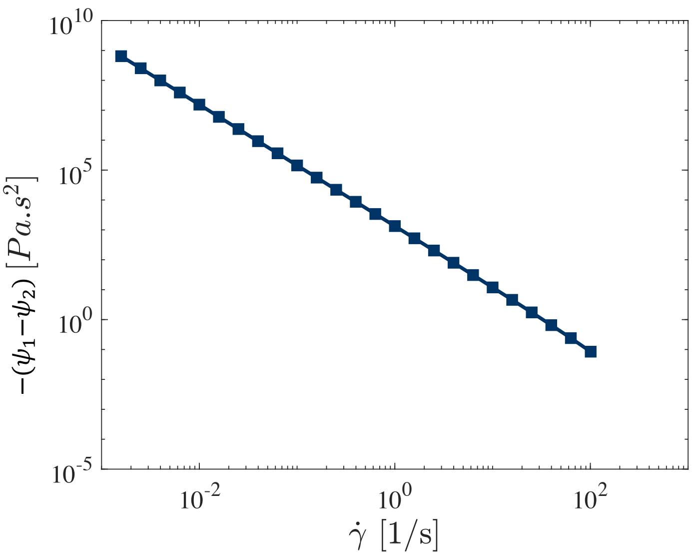

Figure 4.33: Bozzano hair gel (Solar protection):normal stress coefficient *versus* shear rate

Constant shear rate experiments will be discussed in the second part of this section's analysis. The values of shear rate chosen for this study were 100 s^{-1}, 10 s^{-1}, 1 s^{-1}, 0.1 s^{-1} and 0.01 s^{-1}.

Figure 4.34 illustrates a comparison between dynamic and static data for the Bozzano hair gel (Solar protection). Absolute $N_1 - N_2$ were plotted against shear rate for this analysis. Flow curve results studied in the first part of this section construct the dynamic data curve. The static curve is formed of the steady-state values of $N_1 - N_2$ taken from each constant shear rate test. Error bars are assembled from three experiments of each type of test. It is important to mention that flow curve results were submitted to the nonhomogeneous correction, while constant shear rate tests were not.

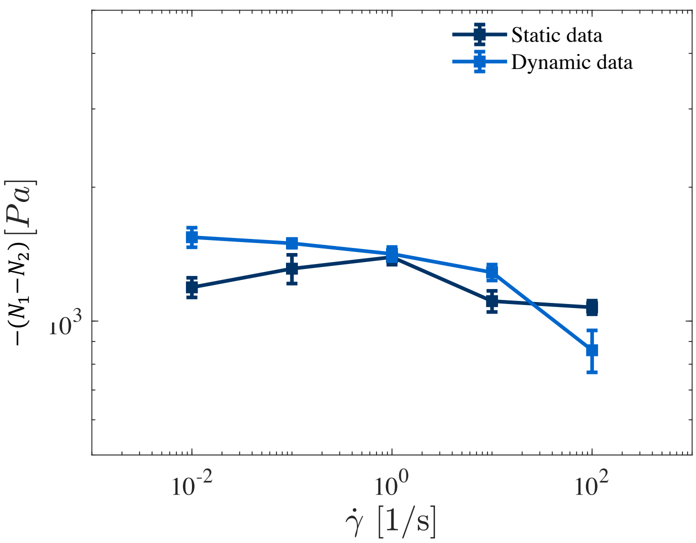

Figure 4.34: Bozzano hair gel (Solar protection): normal stress differences *versus* shear rate for constant shear rate tests and a flow curve test

Analogous to results obtained for the Carpobol dispersion in section 4.2, both static and dynamic data present similar N_1 values. The exception lies mainly in the $N_1 - N_2$ value found for the lowest shear rate, 0.01 s^{-1}. In addition, although the N_1 values for both static and dynamic curves show good repeatability, unmatching results are found when comparing them both. Apparently, the value measured in the flow curve has not reached steady-state, as it took the maximum time to obtain. Data show comparable results when compared at similar time scales.

Constant shear rate experiments of values of 100 s^{-1},10 s^{-1}, 1 s^{-1},0.1 s^{-1} and 0.01 s^{-1} were used to assemble the graph in figure 4.35. Shear stress was plotted against time. It is essential to mention that these plots have not been submitted to the nonhomogeneous correction. Therefore shear stress values differ from those found in the flow curves results discussed previously in this section. Analogous to what was seen for both the highly concentrated emulsion and the Carbopol dispersion, as shear rate increases, the time it takes for stress values to arrive at steady-state reduces. As expected, $N_1 - N_2$ curves found for 1 s^{-1} and 0.1 s^{-1} fall into the same N_1 value after reaching steady-state. The 0.01 s^{-1} appears to not have reached the steady-state regime, which agrees with the results seen in figure 4.34.

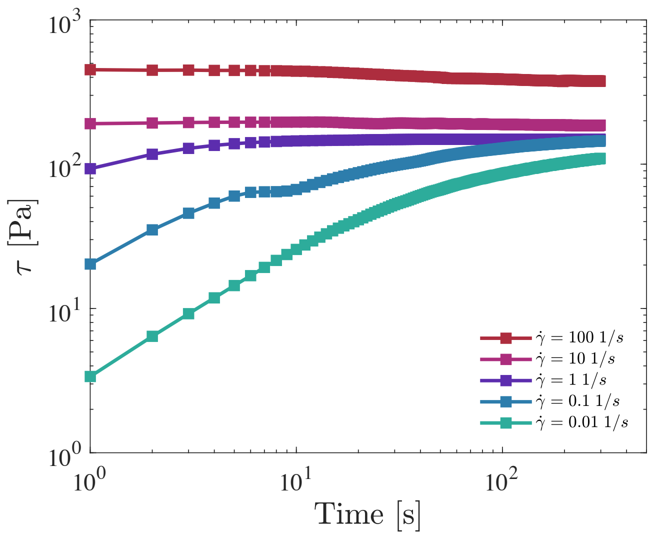

Figure 4.35: Bozzano hair gel (Solar protection): stress *versus* time

Figure 4.36 exhibits the absolute values of $N_1 - N_2$ plotted against time for the constant shear rate experiments. The results of constant shear rate experiments of values of 100 s^{-1},10 s^{-1}, 1 s^{-1}, 0.1 s^{-1} and 0.01 s^{-1} were presented in this graph. As seen in figure 4.35, as shear rate decreases, the time it takes for the steady-state to arrive grows larger. While, in contrast, for all constant shear rate experiments studied, the time it takes to reach a steady-state regime in the normal direction is extremely higher. Further, analogous to what was seen at the beginning of this section, absolute $N_1 - N_2$ values are considerably higher than those found for shear stress. The Carpobol gel and the highly concentrated emulsion were also seen in the discussion surrounding both flow curve and constant shear rate experiments.

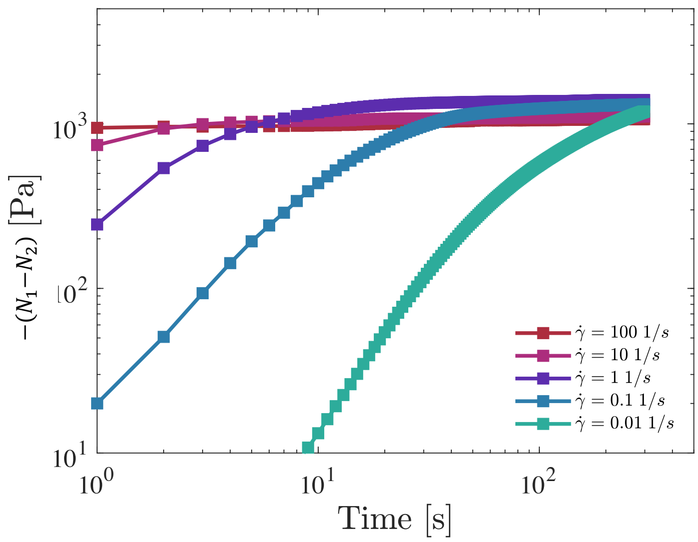

Figure 4.36: Bozzano hair gel (Solar protection): normal stress differences *versus* time (linear plot)

$\psi_1 - \psi_2$ is plotted against time in figure 4.37. For all shear rate values, a plateau is formed that illustrates the behavior of the normal stress coefficient in the log-log plot. As seen for both the Carbopol dispersion and the highly concentrated emulsion in previous sections, the absolute normal stress coefficient values increase as the shear rate decreases. The same was observed in the flow curve results discussed in this section.

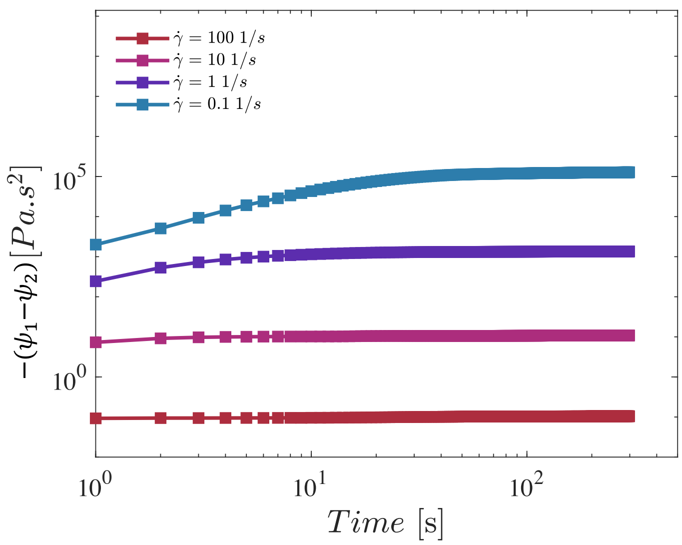

Figure 4.37: Bozzano hair gel (Solar protection): normal stress coefficient *versus* time

4.5 Additional analysis

The previous sections performed an analysis surrounding normal stresses in three different yield stress materials, a Carpobol dispersion, a highly concentrated emulsion, and a commercial hair gel.

As seen in figure 4.38, the three materials present different flow curve results. Although all fluids are yield stress materials and can be fitted in Herschell-Bulkley model, each curve studied shows a particular behavior. High shear stresses were seen for the Bozanno hair gel (Solar protection) under prolonged flow. These values were not as high for the Carpobol dispersion. A wide range of shear stress values was obtained for the highly concentrated emulsion in this study. These results were key to raising interest to investigate $N_1 - N_2$ for these three different yield stress materials.

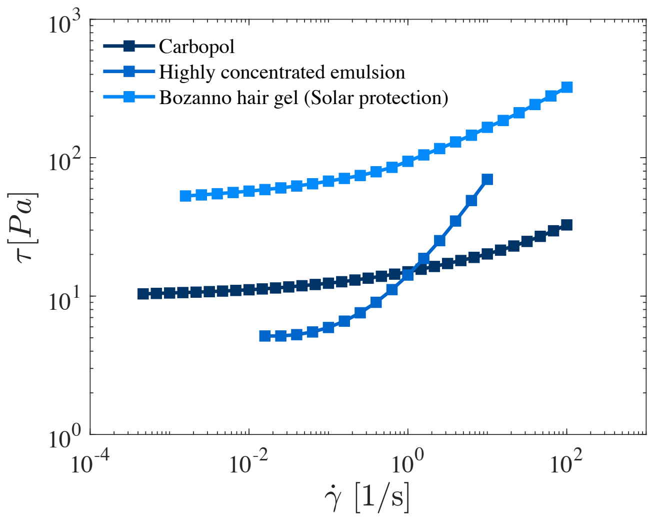

Figure 4.38: Flow curves of the three materials

When comparing $N_1 - N_2$ curves for all three materials studied in this work, shown in figure 4.39, the commercial hair gel also presents the highest $N_1 - N_2$ values in magnitude. All curves display similar behavior at the beginning of the test, starting with lower stresses. These stresses either increase or form a plateau as shear rate decreases and the materials are submitted to continuous flow. Interestingly, in contrast to what was seen in figure 4.38, the results obtained for highly concentrated emulsion and the Carpobol dispersion are extremely distant in the normal stress analysis.

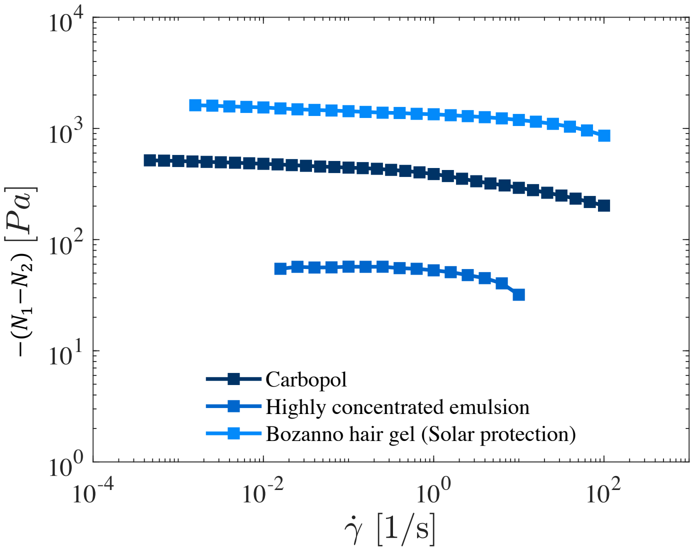

Figure 4.39: Normal stress differences curves of the three materials

Finally in figure 4.40, N_1 is plotted against $(\tau - \tau_y)/\tau$ for all three materials. This plot contrasts with what was seen in literature in works done for yield stress materials (27) and non-Brownian Suspensions (37), in which for all systems, $N_1 - N_2$ depends linearly on $\tau - \tau_y$. In the present work, the three materials studied present no common dependence for the two parameters studied. The commercial hair gel presents a non linear dependence between the $N_1 - N_2$ value and the normalized shear stress. While the other two, display a linear curve, but with completly different inclinations. Also, the magnitudes of the values obtained are quite different for the Carpobol dispersion, highly concentrated emulsion, and Bozanno hair gel (Solar protection).

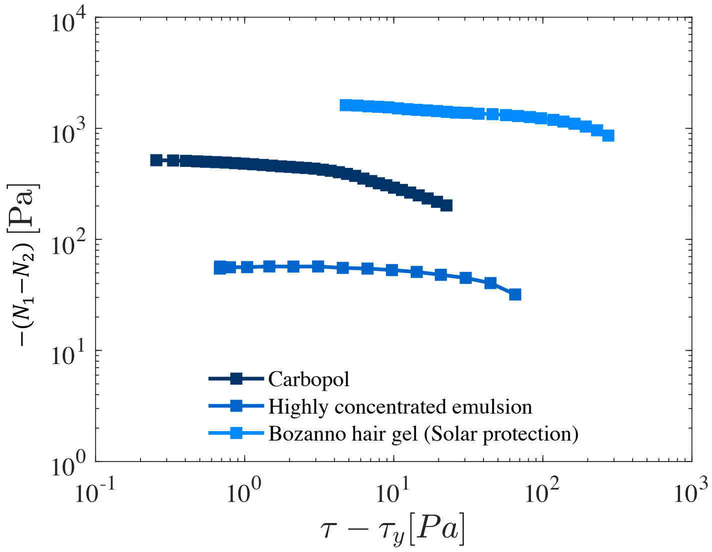

Figure 4.40: Normal stress differences curves of the three materials normalized shear stress

4.6
Von Mises criterion analysis

A quick look into the Von Mises criterion will be taken in this part of the work. The contribution of the normal stress in this criterion is usually neglected. The idea of this work is to discuss the validity this common approach. Firstly, the Von Mises criterion will be tested for the materials studied for the highest and lowest normal stress value (and their respective shear stress). Finally, a comparison between the normal and shear stress contributions in the Von Mises inequality will be presented.

It is important to point out this is an approximate study of the Von Mises criterion. This work uses a parallel plate geometry and the values of $N_1 - N_2$ are the ones analysed. For that account, two different N_2 relationship were studied. Firstly, N_2 values are set to zero as for an ideal rubber for the purpose of this quick analysis. Then, N_2 values were set to $N_2 = -N_1$.

For a simple shear flow, with flow in the 1-direction, flow gradient in the 2-direction, and vorticity in the 3-direction, the Von Mises yield criterion can be written as:

$$N_1^2 + N_2^2 + (N_1 + N_2)^2 + 6\tau^2 \geq 2\sigma_y^2 \quad (35) \qquad \text{(4-3)}$$

In this criterion, σ_y is calculated according to the following equation (73):

$$\sigma_y = \sqrt{\tau_y^2 + \frac{1}{3}\,(N_{1,y}^2 + N_{1,y}\,N_{2,y} + N_{2,y}^2)} \tag{4-4}$$

The Carpobol dispersion and the highly concentrated emulsion were fitted to the Herschell-Bulkley model and $N_{1,y} - N_{2,y}$ values were found for both materials. They were then used for this Von Mises analysis.

For the Carpobol dispersion, $N_{1,y} - N_{2,y}$ was -598 Pa and τ_y was 10.125 Pa. Using these values, σ_y was calculated. For $N_2 = 0$:

$$\sigma_y = \sqrt{(10.125)^2 + \tfrac{1}{3}\,((-598)^2 + (-598)\,0 + 0)} = 345\,Pa$$

And for $N_2 = -N_1$:

$$\sigma_y = \sqrt{(10.125)^2 + \tfrac{1}{3}\,((-299)^2 + (-299)\,(299) + 299^2)} = 173\,Pa$$

The highest value of $N_1 - N_2$ was -280 Pa and the lowest was -500 Pa. Both values and their respective shear stress values are represented by the letters *h* and *l*. These values were put in the Von Mises Criterion as follows:

$$N_{1h} - N_{2h} = -280\ Pa \text{ and } N_{1l} - N_{2l} = -500\ Pa$$

For $N_2 = 0$:

$$N_{1h} = -280\ Pa,\ \tau_h = 20\ Pa \text{ e } N_{2h} = 0\ Pa$$
$$N_{1l} = -500\ Pa,\ \tau_l = 11\ Pa \text{ e } N_{2l} = 0\ Pa$$

For the highest value of normal stress:

$$N_{1h}^2 + N_{2h}^2 + (N_{1h} + N_{2h})^2 = 156800\ Pa^2$$
$$6\tau_h^2 = 2400\,Pa^2$$
$$N_{1h}^2 + N_{2h}^2 + (N_{1h} + N_{2h})^2 + 6\tau_h^2 = 159200\,Pa^2$$
$$2\sigma_y^2 = 238050\ Pa^2$$

For the lowest value of normal stress:

$$N_{1l}^2 + N_{2l}^2 + (N_{1l} + N_{2l})^2 = 500000\ Pa^2$$
$$6\tau_l^2 = 726\ Pa^2$$
$$N_{1l}^2 + N_{2l}^2 + (N_{1l} + N_{2l})^2 + 6\tau_l^2 = 500726\,Pa^2$$

$$2\sigma_y^2 = 238050\ Pa^2$$

According to the approximate results obtained for the Carpobol dispersion, the Von Mises Criterion indicates yielding for the lowest value of normal stress since the left part of equation 4-4 is greater than the right one. The shear stress value at this point was 11 Pa, which is approximately the yield stress of the Carpobol fluid. For the highest normal stress value, the opposite was obtained. For a shear stress greater than the yield stress (indicating the material is under flow), the left part of the equation was smaller than the other part. Therefore, this would not be a valid criterion for this material.

For $N_2 = -N_1$:

$$N_{1h} = -140\ Pa,\ \tau_h = 20\ Pa \text{ e } N_{2h} = 140\ Pa$$
$$N_{1l} = -250\ Pa,\ \tau_l = 11\ Pa \text{ e } N_{2l} = 250\ Pa$$

For the highest value of normal stress:

$$N_{1h}^2 + N_{2h}^2 + (N_{1h} + N_{2h})^2 = 39200\ Pa^2$$
$$6\tau_h^2 = 2400\ Pa^2$$
$$N_{1h}^2 + N_{2h}^2 + (N_{1h} + N_{2h})^2 + 6\tau_h^2 = 41600\ Pa^2$$
$$2\sigma_y^2 = 59881\ Pa^2$$

For the lowest value of normal stress:

$$N_{1l}^2 + N_{2l}^2 + (N_{1l} + N_{2l})^2 = 125000\ Pa^2$$
$$6\tau_l^2 = 726\ Pa^2$$
$$N_{1l}^2 + N_{2l}^2 + (N_{1l} + N_{2l})^2 + 6\tau_l^2 = 125726\ Pa^2$$
$$2\sigma_y^2 = 59881\ Pa^2$$

As was seen for the $N_2 = 0$ results, the Von Mises Criterion indicates yielding for the lowest value of normal stress differences and not for the highest value of normal stress differences. Hence, this would not be a valid criterion for this material.

The same analysis was done for the highly concentrated emulsion.$N_{1,y} - N_{2,y}$ was -58 Pa and τ_y was 4.47 Pa. Using these values, σ_y was calculated. Firstly, σ_y was calculated for $N_2 = 0$:

$$\sigma_y = \sqrt{(4.468)^2 + \frac{1}{3}\left((-58.5)^2 + (-58.5)\,0 + 0\right)} = 34.05\ Pa$$

And for $N_2 = -N_1$:

$$\sigma_y = \sqrt{(4.468)^2 + \frac{1}{3}\left((-58.5)^2 + (-58.5)\,58.5 + 58.5^2\right)} = 17.45\,Pa$$

The values chosen for this quick study were:

$N_{1h} - N_{2h} = -38\ Pa$, $N_{1i} - N_{2i} = -55\ Pa$ and $N_{1l} - N_{2l} = -58\ Pa$

For $N_2 = 0$:
$N_{1h} = -38\ Pa$, $\tau_h = 49\ Pa$ e $N_{2h} = 0\ Pa$
$N_{1i} = -55\ Pa$, $\tau_i = 6.7\ Pa$ e $N_{2i} = 0\ Pa$
$N_{1l} = -58\ Pa$, $\tau_l = 2\ Pa$ e $N_{2l} = 0\ Pa$
For the highest value of normal stress:

$N_{1h}^2 + N_{2h}^2 + (N_{1h} + N_{2h})^2 = 2888\ Pa^2$
$6\tau_h^2 = 14406\ Pa^2$
$N_{1h}^2 + N_{2h}^2 + (N_{1h} + N_{2h})^2 + 6\tau_h^2 = 17294\,Pa^2$
$2\sigma_y^2 = 2318\ Pa^2$

For the intermediate value of normal stress:

$N_{1i}^2 + N_{2i}^2 + (N_{1i} + N_{2i})^2 = 6050\ Pa^2$
$6\tau_i^2 = 269\ Pa^2$
$N_{1i}^2 + N_{2i}^2 + (N_{1i} + N_{2i})^2 + 6\tau_i^2 = 6319\,Pa^2$
$2\sigma_y^2 = 2318\ Pa^2$

For the lowest value of normal stress:

$N_{1l}^2 + N_{2l}^2 + (N_{1l} + N_{2l})^2 = 6835\ Pa^2$
$6\tau_l^2 = 24\ Pa^2$
$N_{1l}^2 + N_{2l}^2 + (N_{1l} + N_{2l})^2 + 6\tau_l^2 = 6859\,Pa^2$
$2\sigma_y^2 = 2318\ Pa^2$

For the highly concentrated emulsion and $N_2 = 0$, even for values of shear stress below the yield stress, the Von Mises criterion indicates yielding. For all values studied, the left part of equation 4-4 is greater than the right one.

For $N_2 = -N_1$:
$N_{1h} = -19\ Pa$, $\tau_h = 49\ Pa$ e $N_{2h} = 19\ Pa$
$N_{1i} = -27.5\ Pa$, $\tau_i = 6.7\ Pa$ e $N_{2i} = 27.5\ Pa$

$N_{1l} = -29\ Pa$, $\tau_l = 2\ Pa$ e $N_{2l} = 29\ Pa$

For the highest value of normal stress:

$N_{1h}^2 + N_{2h}^2 + (N_{1h} + N_{2h})^2 = 722\ Pa^2$
$6\tau_h^2 = 14406\ Pa^2$
$N_{1h}^2 + N_{2h}^2 + (N_{1h} + N_{2h})^2 + 6\tau_h^2 = 15128\ Pa^2$
$2\sigma_y^2 = 609\ Pa^2$

For the intermediate value of normal stress:

$N_{1i}^2 + N_{2i}^2 + (N_{1i} + N_{2i})^2 = 1512\ Pa^2$
$6\tau_i^2 = 269\ Pa^2$
$N_{1i}^2 + N_{2i}^2 + (N_{1i} + N_{2i})^2 + 6\tau_i^2 = 1781\ Pa^2$
$2\sigma_y^2 = 609\ Pa^2$

For the lowest value of normal stress:

$N_{1l}^2 + N_{2l}^2 + (N_{1l} + N_{2l})^2 = 1708\ Pa^2$
$6\tau_l^2 = 24\ Pa^2$
$N_{1l}^2 + N_{2l}^2 + (N_{1l} + N_{2l})^2 + 6\tau_l^2 = 1732\ Pa^2$
$2\sigma_y^2 = 609\ Pa^2$

As observed for the for the highly concentrated emulsion and $N_2 = 0$, even for values of shear stress below the yield stress, the Von Mises criterion indicates yielding. Thus, this criterion is not applicable for this fluid.

The commercial hair gel was left out of this study because a $N_{1,y}$ could not be obtained. This small analysis elucidates the importance of better understanding the stress state in yield stress materials. The normal stress contribution in the commonly used Von Mises criterion is extremely significant and should not be neglected. By neglecting normal stress contributions, most works are simply comparing the influences of the shear stresses, although this can not be defined as the Von Mises criterion. The analysis exemplified by these two fluids displays the challenging and contrasting results found against those presented in literature.

5 Final remarks

The study of the normal forces when fluids undergo shear flow started with Weissenberg, and this field has developed largely ever since. The interest in normal stresses for yield stress materials arose not long ago, consequently the few studies that investigate this phenomenon are promising but not yet conclusive.

In order to obtain a complete description of the behavior of an elastoviscoplastic fluid, it is essential to characterize the full tensorial stress state. To fully understand the stress tensor of these complex fluids, the shear stress values, τ, the first and second normal stress difference, N_1 and N_2, should be investigated. Many works were done investigating parameters in the direction of the flow of these materials, but not many studied the normal direction.

This gap calls for more study surrounding the normal direction for viscoplastic materials. To this end, many research groups worldwide have proposed different methods for measuring and analyzing the effects of normal stresses for elastoviscoplastic materials.

In this work, a novel methodology for the rheological characterization of the results for normal forces of viscoplastic materials under shear deformation is proposed. A TA Instrument's strain-controlled rheometer was chosen to perform these measurements due to the effectiveness of its normal force transducer. As for the viscoplastic material, a Carpobol dispersion, a highly concentrated emulsion, and a commercial hair gel were selected, and different rheometric experiments were performed for an interesting analysis around the behavior of the material at hand.

Flow curves and constant shear rate tests were performed to characterize these materials. Interesting results were found when considering flow curve tests for the materials studied. Only negative normal stress results were obtained, contrasting with most results found in literature. The normal stress curves for the Carbopol dispersion and the highly concentrated hair gel were fitted to a Herschell-Bulkley model, and a finite value of the parameter τ_{N_y} was found, suggesting the existence of a "yield normal stress". However, the same trend was not seen for the Bozanno hair gel (Solar protection). Normal stresses higher than shear stresses were observed for all three materials at low shear rates. This behavior changes for high shear rates for the highly concentrated emulsion studied.

Compelling plots of ψ_1 show the behavior of this parameter was analogous to those found in literature when its absolute value was plotted. Results obtained from flow curve and constant shear rate experiments were compared. The curves for the static and dynamic data for the Carpobol dispersion and the commercial hair gel displayed similar results. The relationship between these two curves elucidates the complexity surrounding normal stress measurements.

It was found that the normal residual stresses of the elasto-viscoplastic material studied can deeply influence the repeatability of the results for normal force measurements. In order to reduce or eliminate these effects, different pre-test procedures were suggested, and an effective procedure was developed to perform flow curve experiments. Among other findings, it was found that the time needed to reach a steady-state while measuring normal stresses is longer than that of the shear properties of yield stress materials.

Finally, a quick study of the Von Mises equation was performed to investigate the weight of the normal stress contribution and the applicability of the criterion for two of the materials studied. For the Carpobol dispersion, the criterion indicated not yielding for shear stress values above the yield stress. While for the highly concentrated emulsion, the Von Mises criterion indicated yielding for all shear stress values, even below the yield stress. The criterion was found not to apply in the analysis performed. Also, significant normal stress contributions were obtained, illustrating that this parameter should not be neglected.

Future work includes a better understanding of the contribution of the interfacial tension in normal stress measurements for yield stress materials. Another important step would be to study the second normal stress differences in the tests for the materials analyzed in this work. Many works in literature investigate the behavior of the two normal stress parameters.

Moreover, it would be interesting to analyze different elastoviscoplastic materials to compare their normal force behavior to the one found for the fluids studied in this work. Indeed, drilling fluids were already tested in this project before the choice to study the three viscoplastic materials and showed interesting normal stress responses that could be better investigated.

Bibliography

[1] A. N. BERIS, J. A. TSAMOPOULOS, R. C. A.; BROWN, R. A.. **Creeping motion of a sphere through a bingham plastic**. Journal of Fluid Mechanics, 158(1):219, 1985.

[2] A. SHAUKAT, M. KAUSHAL, A. S.; JOSHI, Y. M.. **Shear mediated elongational flow and yielding in soft glassy materials**. Soft Matter, 8(39):10107, 2012.

[3] AHMED, E. M.. **Hydrogel: Preparation, characterization, and applications: A review**. Journal of Advanced Research, 6(2):105 – 121, 2015.

[4] AHONGUIO, F., L. J.; MAGNIN, A.. **Influence of surface proper- ties on the flow of a yield stress fluid around spheres**. Journal of Non-Newtonian Fluid Mechanics, 206:57–70, 2014.

[5] ALCOUTLABI, M.; BAEK, S. G.; MAGDA, J. J.; SHI, X.; HUTCHESON, S. A. ; MCKENNA, G. B.. **A comparison of three different methods for measuring both normal stress differences of viscoelastic liquids in torsional rheometers**. Rheologica Acta, 48(2):191–200, 2009.

[6] BAGLEY, E.; DUFFEY, H.. **Recoverable shear strain and the barus effect in polymer extrusion**. Journal of Rheology, 14(4), 1970. cited By 68.

[7] BAIRD, D. G.. **First normal stress difference measurements for polymer melts at high shear rates in a slit-die using hole and exit pressure data**. Journal of Non-Newtonian Fluid Mechanics, 148(1):13 – 23, 2008. The A.S. Lodge Commemorative Meeting on Rheometry.

[8] BARNES, H. A.. **The yield stress-a review or $\pi\alpha\nu\tau\alpha\ \rho\epsilon\iota$ -everything flows?** Journal of Non-Newtonian Fluid Mechanics, 81(1):133–178, 1999.

[9] BARNES, H. A.. **A Handbook of Elementary Rheology**. University of Wales, 2000.

[10] BINGHAM, E. C.. **Rheology. i. the nature of fluid flow**. Journal of Chemical Education, 6(6):1113, 06 1929.

[11] BIRD, R. B.; ARMSTRONG, R. C. ; HASSAGER, O.. **Dynamics of Polymeric Liquids**. John Wiley & Sons, New York, second edition, 1987. vol. 1.

[12] BOGER, D.; WALTERS, K.. **Rheological Phenomena in Focus**. Elsevier, 1993.

[13] BRADER, J.; VOIGTMANN, T.; FUCHS, M.; LARSON, R. ; CATES, M.. **Glass rheology: From mode-coupling theory to a dynamical yield criterion**. Proceedings of the National Academy of Sciences of the United States of America, 106:15186–91, 09 2009.

[14] BUSCALL, R.; MCGOWAN, J. I. ; MORTON-JONES, A. J.. **The rheology of concentrated dispersions of weakly attracting colloidal particles with and without wall slip**. Journal of Rheology, 37(4):621–641, 1993.

[15] CALADO, V. M. A.; WHITE, J. M. ; MULLER, S. J.. **Transient behavior of boger fluids under extended shear flow in a cone-and-plate rheometer**. Rheologica Acta, 44(3):250–261, Jan 2005.

[16] CARNALI, J. O.; NASER, M. S.. **The use of dilute solution viscometry to characterize the network properties of carbopol microgels**. Colloid and Polymer Science, 270(2):183–193, 1992.

[17] CATO, A. D.; EDIE, D. D. ; HARRISON, G. M.. **Steady state and transient rheological behavior of mesophase pitch, part i: Experiment**. Journal of Rheology, 49(1):161–174, 2005.

[18] COUSSOT, P.. **Yield stress fluid flows: A review of experimental data**. Journal of Non-Newtonian Fluid Mechanics, 211:31 – 49, 2014.

[19] COUSSOT, P.; TOCQUER, L.; LANOS, C. ; OVARLEZ, G.. **Macroscopic vs. local rheology of yield stress fluids**. Journal of Non-Newtonian Fluid Mechanics, 158(1):85 – 90, 2009. Visco-plastic fluids: From theory to application.

[20] DBOUK, T.; LOBRY, L. ; LEMAIRE, E.. **Normal stresses in concentrated non-brownian suspensions**. Journal of Fluid Mechanics, 715:239–272, 2013.

[21] DE CAGNY, H.; FAZILATI, M.; HABIBI, M.; DENN, M. M. ; BONN, D.. **The yield normal stress**. ArXiv e-prints, 2018.

[22] DE CAGNY, H.; FAZILATI, M.; HABIBI, M.; DENN, M. M. ; BONN, D.. **The yield normal stress**. Journal of Rheology, 63(2):285–290, 2019.

[23] DE CAGNY, H. C. G.; VOS, B. E.; VAHABI, M.; KURNIAWAN, N. A.; DOI, M.; KOENDERINK, G. H.; MACKINTOSH, F. C. ; BONN, D.. **Porosity governs normal stresses in polymer gels**. Phys. Rev. Lett., 117:217802, Nov 2016.

[24] DE SOUZA MENDES, P.; ALICKE, A. ; THOMPSON, R.. **Parallel-plate geometry correction for transient rheometric experiments**. Applied Rheology, 24:52721, 10 2014.

[25] DE SOUZA MENDES, P. R.; NACCACHE, M. F.; VARGES, P. R. ; MARCHESINI, F. H.. **Flow of viscoplastic liquids through axisymmetric expansions-contractions**. J. Non-Newtonian Fluid Mech., 142(1-3):207–217, 2007.

[26] DI GIUSEPPE, E.; CORBI, F.; FUNICIELLO, F.; MASSMEYER, A.; SANTIMANO, T.; ROSENAU, M. ; DAVAILLE, A.. **Characterization of carbopol® hydrogel rheology for experimental tectonics and geodynamics**. Tectonophysics, 642:29 – 45, 2015.

[27] FAZILATI, M.; HABIBI, M. ; BONN, D.. **Normal stresses in yield stress fluid**. Sent to RSC Advances on 31-Aug-17.

[28] FRAGGEDAKIS, D.; DIMAKOPOULOS, Y. ; TSAMOPOULOS, J.. **Yielding the yield-stress analysis: a study focused on the effects of elasticity on the settling of a single spherical particle in simple yield-stress fluids**. Soft Matter, 12:5378–5401, 2016.

[29] FRANCK, A.. **Normal stresses in shear flow**. Technical report, TA Instruments, 2007.

[30] FRIGAARD, I.. **Simple yield stress fluids**. Current Opinion in Colloid Interface Science, 43:80 – 93, 2019. Rheology.

[31] G. OVARLEZ, Q. B.; COUSSOT, P.. **Three-dimensional jamming and flows of soft glassy materials**. Nature Materials, 9(2):115–119, 2010.

[32] GADALA-MARIA, F. A.. **The rheology of concentrated suspensions**. Tese de Doutorado, Stanford University, 1979.

[33] GARLAND, S.; GAUTHIER, G.; MARTIN, J. ; MORRIS, J. F.. **Normal stress measurements in sheared non-brownian suspensions**. Journal of Rheology, 57(1):71–88, 2013.

[34] H.A. BARNES, J. H.; F.R.S, K. W.. **An Introduction to Rheology**. Elsevier, 1989.

[35] HABIBI, M.; DINKGREVE, M.; PAREDES, J.; DENN, M. ; BONN, D.. **Normal stress measurement in foams and emulsions in the presence of slip**. Journal of Non-Newtonian Fluid Mechanics, 238:33 – 43, 2016. Viscoplastic Fluids From Theory to Application 2015 (VPF6).

[36] HERSCHEL, W. H.; BULKLEY, R.. **Konsistenzmessungen von gummibenzollösungen**. Kolloid-Zeitschrift, 39(4):291–300, 1926.

[37] I. E. ZARRAGA, D. A. H.; JR, D. T. L.. **The characterization of the total stress of concentrated suspensions of noncolloidal spheres in newtonian fluids**. Journal of Rheology, 44(2):185–220, 2000.

[38] J. PAREDES, M. A. J. M.; BONN, D.. **Rheology across the zero-temperature jamming transition,**. Phys. Rev. Lett., 111(1):015701, 2013.

[39] JANMEY, P. A.; MCCORMICK, M. E.; RAMMENSEE, S.; LEIGHT, J. L.; GEORGES, P. C. ; MACKINTOSH, F. C.. **Negative normal stress in semiflexible biopolymer gels**. Nature Materials, 6:48 EP –, 12 2006.

[40] JOMHA, A. I.; REYNOLDS, P. A.. **An experimental study of the first normal stress difference — shear stress relationship in simple shear flow for concentrated shear thickening suspensions**. Rheologica Acta, 32(5):457–464, Sep 1993.

[41] JØRGENSEN, L.; LE MERRER, M.; DELANOË-AYARI, H. ; BARENTIN, C.. **Yield stress and elasticity influence on surface tension measurements**. Soft Matter, 11:5111–5121, 2015.

[42] KABLA, A.; DEBREGEAS, G.. **Quasi-static rheology of foams. part 1. oscillating strain**. Journal of Fluid Mechanics, 587:23–44, 2007.

[43] KABLA, A.; SCHEIBERT, J. ; DEBREGEAS, G.. **Quasi-static rheology of foams. part 2. continuous shear flow**. Journal of Fluid Mechanics, 587:45–72, 2007.

[44] KISS, G.; PORTER, R. S.. **Rheology of concentrated solutions of poly(-benzyl-glutamate)**. Journal of Polymer Science: Polymer Symposia, 65(1):193–211, 1978.

[45] KOLLI, V. G.; POLLAUF, E. J. ; GADALA-MARIA, F.. **Transient normal stress response in a concentrated suspension of spherical particles**. Journal of Rheology, 46(1):321–334, 2002.

[46] LABIAUSSE, V.; HÖHLER, R. ; COHEN-ADDAD, S.. **Shear induced normal stress differences in aqueous foams**. Journal of Rheology, 51(3):479–492, 2007.

[47] LAUN, H.. **Normal stresses in extremely shear thickening polymer dispersions**. Journal of Non-Newtonian Fluid Mechanics, 54:87 – 108, 1994.

[48] LEOPERCIO, B. C.. **Cinética da formação de hidrato de ciclopentano: Um estudo da reologia interfacial**. Dissertação de Mestrado, PONTIFÍCIA UNIVERSIDADE CATÓLICA DO RIO DE JANEIRO - PUC-RIO, 2017.

[49] MACDONALD, M. J.; MULLER, S. J.. **Shear rheology of polymer solutions near the critical condition for elastic instability**. Rheologica Acta, 36(2):97–109, 1997.

[50] MACOSKO, C. W.. **RHEOLOGY Principles, Measurements and Applications**. WILEY-VCH, 1994.

[51] MALKIN, A. Y.. **Rheology Fundamentals**. ChemTec Publishing, 1994.

[52] MALKIN, A. Y.; MASALOVA, I.. **Shear and normal stresses in flow of highly concentrated emulsions**. Journal of Non-Newtonian Fluid Mechanics, 147(1):65 – 68, 2007.

[53] MAO, B.; DIVOUX, T. ; SNABRE, P.. **Normal force controlled rheology applied to agar gelation**. Journal of Rheology, 60(3):473–489, 2016.

[54] MARCHESINI, F. H.; ALICKE, A. A.; DE SOUZA MENDES, P. R. ; ZIGLIO, C. M.. **Rheological characterization of waxy crude oils: Sample preparation**. Energy & Fuels, 26(5):2566–2577, 05 2012.

[55] MASALOVA, I.; FABRICE, K. K.; TSHILUMBU, N. N.; GEORGE, N. ; MALKIN, A. Y.. **Emulsification of highly concentrated emulsions—a criterion of shear stability**. Journal of Rheology, 62(3):781–790, 2018.

[56] MASALOVA, I.; TAYLOR, M.; KHARATIYAN, E. ; MALKIN, A. Y.. **Rheopexy in highly concentrated emulsions**. Journal of Rheology, 49(4):839–849, 2005.

[57] METZNER, A. B.; FEEHS, R. H.; RAMOS, H. L.; OTTO, R. E. ; TUTHILL, J. D.. **Agitation of viscous newtonian and non-newtonian fluids**. AIChE Journal, 7(1):3–9, 1961.

[58] MONTESI, A., A. A. P.; PASQUALI, M.. **Vorticity alignment and negative normal stresses in sheared attractive emulsions,**. Phys. Rev. Lett., 92(5):058303, 2004.

[59] MORTON E. GURTIN, E. F.; ANAND, L.. **The Mechanics and Thermodynamics of Continua**. Cambridge University Press, 2010.

[60] NAKAJIMA, N.; HARRELL, E. R.. **Normal stresses in flow of polyvinyl chloride plastisols**. Journal of Applied Polymer Science, 103(5):2769–2775, 2007.

[61] NELSON, A. Z.; BRAS, R. E.; LIU, J. ; EWOLDT, R. H.. **Extending yield-stress fluid paradigms**. Journal of Rheology, 62(1):357–369, 2018.

[62] NIEMIEC, J. M.; PESCE, J.; MCKENNA, G. B.; SKOCYPEC, S. ; GARRITANO, R. F.. **Anomalies in the normal force measurement when using a force rebalance transducer**. Journal of Rheology, 40(3):323–334, 1996.

[63] OHL, N.; GLEISSLE, W.. **The second normal stress difference for pure and highly filled viscoelastic fluids**. Rheologica Acta, 31(3):294–305, May 1992.

[64] OVARLEZ, G.; COHEN-ADDAD, S.; KRISHAN, K.; GOYON, J. ; COUSSOT, P.. **On the existence of a simple yield stress fluid behavior**. Journal of Non-Newtonian Fluid Mechanics, 193:68 – 79, 2013. Viscoplastic Fluids: From Theory to Application.

[65] PAN, Z.; DE CAGNY, H.; HABIBI, M. ; BONN, D.. **Normal stresses in shear thickening granular suspensions**. Soft Matter, 13:3734–3740, 2017.

[66] PIAU, J. M.. **Carbopol gels: Elastoviscoplastic and slippery glasses made of individual swollen sponges. meso- and macroscopic proper- ties, constitutive equations and scaling laws**. Journal of Non-Newtonian Fluid Mechanics, 144(1):1–29, 2007.

[67] RILEY, W.; STURGES, L. ; MORRIS, D.. **Mechanics of Materials**. Wiley, 1998.

[68] S. A. KHAN, C. A. S.; ARMSTRONG, R. C.. **Foam rheology: Iii. measurement of shear flow properties**. Journal of Rheology, 32(5):69–92, 1988.

[69] SCHULTESIZ, C. R.; MCKENNA, G.. **Thermal expansion and its effect on the normal force for a modified force rebalance transducer**. 1999.

[70] SCHWEIZER, T.. **Measurement of the first and second normal stress differences in a polystyrene melt with a cone and partitioned plate tool**. Rheologica Acta, 41(4):337–344, Jan 2002.

[71] STANDARD, A.. **Standard practice for the preparation of substitute ocean water**, d1141-98 edition, 2013.

[72] THOMPSON, R. L.; DE SOUZA MENDES, P. R.. **Rheological material functions at yielding**. Journal of Rheology, 64(3):615–624, 2020.

[73] THOMPSON, R. L.; SICA, L. U. ; DE SOUZA MENDES, P. R.. **The yield stress tensor**. Journal of Non-Newtonian Fluid Mechanics, 261:211–219, 2018.

[74] VARGES, P.; COSTA, C.; FONSECA, B.; NACCACHE, M. ; DE SOUZA MENDES, P.. **Rheological characterization of carbopol® dispersions in water and in water/glycerol solutions**. Fluids, 4:3, 01 2019.

[75] VERRELLI, D. I.; KILCULLEN, A. R.. **Normal stress differences and yield stresses in attractive particle networks**. Advances in Condensed Matter Physics, 2016(1716598), 2016.

[76] WEN, Q.; BASU, A.; WINER-JONES, J.; YODH, A. ; JANMEY, P.. **Local and global deformations in a strain-stiffening fibrin gel**. New Journal of Physics, 9:428, 11 2007.

[77] YAMAMOTO, T.; MASUBUCHI, Y. ; DOI, M.. **Relaxation dynamics of the normal stress of polymer gels**. Macromolecules, 50(13):5208–5213, 2017.

[78] ZHANG, X.; FADOUL, O.; LORENCEAU, E. ; COUSSOT, P.. **Yielding and flow of soft-jammed systems in elongation**. Phys. Rev. Lett., 120:048001, Jan 2018.

A
Comparison between rugged parallel plate and smooth parallel plate

Rheological measurements for yield stress materials can be affected by apparent wall slip (54). In order to perform measurements for yield stress fluids, it is important to account for wall slip at low strain rates. Rugged geometries can reduce the wall slip effects in the measurements caused by the thin layer of liquid formed at the wall. In this work, it is believed that wall slip will not influence the results of the measurements of normal forces. Flow curves were performed in other to validate this theory.

Figure A.1 shows shear stress *versus* shear rate. It can be seen that both curves, the one made using a rugged geometry and the one made using a smooth geometry, coincide for high shear rates. Although, for low shear rates, the wall slip effects can be seen for the test made with the smooth geometry.

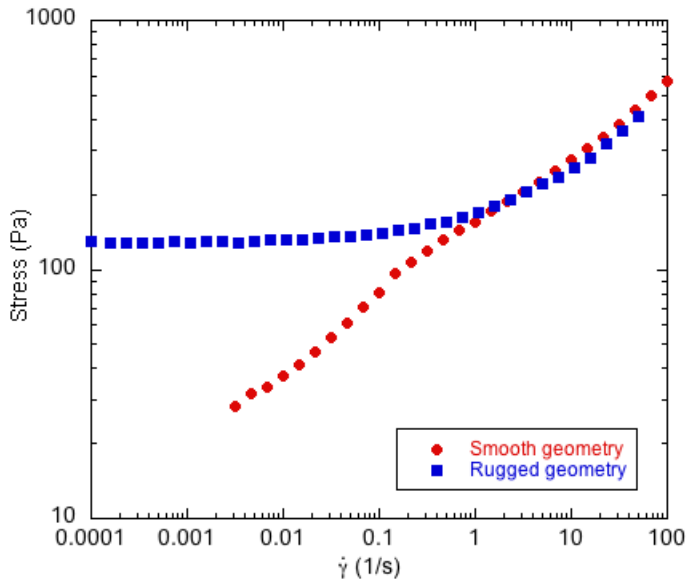

Figure A.1: Flow curve: Shear stress x shear rate

To analyze the effects of the wall slip in the normal direction, the normal force was plotted against the shear rate (figure A.2). As a result, it can be seen that the curves of the test made using a rugged geometry and the one made using a smooth geometry coincide for low and high shear rates, as expected.

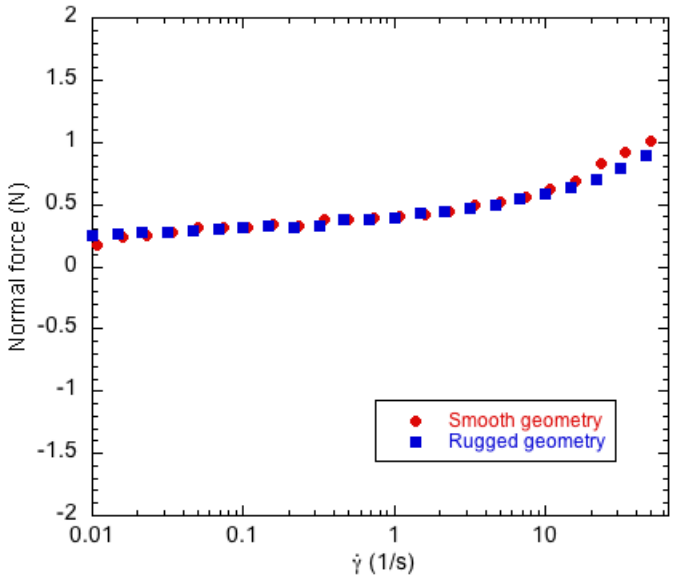

Figure A.2: Flow curve: Normal force x shear rate

B
Pre test procedures

B.1
Details on the pre test procedures in the rheometer

As previously discussed, before each test, the rheometer performed a conditioning transducer step, a conditioning sample step, and a pre-shear step. These steps that must be done have to be set up when preparing the rheometric experiment. Therefore, a more detailed explanation of each step is shown in this section.

According to the manufacturer, a step of conditioning transducer is indicated when measuring normal forces. This conditioning step enables achieving a better motor performance and higher accuracy of the torque and normal force transducers. Figure B.1 shows the conditioning transducer step used to perform the normal force measurements in this work.

In the conditioning transducer step, the normal transducer force mode was switched to Spring Mode. Although switching to FRT, which implies a stiff mode, is recommended to moderate to high viscosity systems and is consequently more precise than Spring mode, the lack of compliance may cause the normal force to jump or increase if the sample is stiff enough. The torque transducer is switched to FRT mode, implying a stiff mode. This set-up was recommended by the manufacturer.

The motor state is set to "locked," which prevents the material from drifting during the sample equilibrium. This motor state leads to introducing a residual torque to the sample at the beginning of the test. The "equilibration" time indicates the time for the material to relax. Once the material is left to relax during the conditioning sample step, a time of 10.0 s seems to be sufficient for this equilibrium delay.

Regarding the range selection for the transducer, the appropriate range depends on the material used and the test performed. This choice is extremely important to avoid loss of torque sensitivity during the rheometric experiment. The manufacturer indicates that the low range should be used for 0.05 to 5000 μ Nm, the med range from 0.4 to 20000 μ Nm and the high range should be from 4 to 200000 μ Nm. The medium-range was selected for all tests in this work. Finally, the torque and normal force are set to zero.

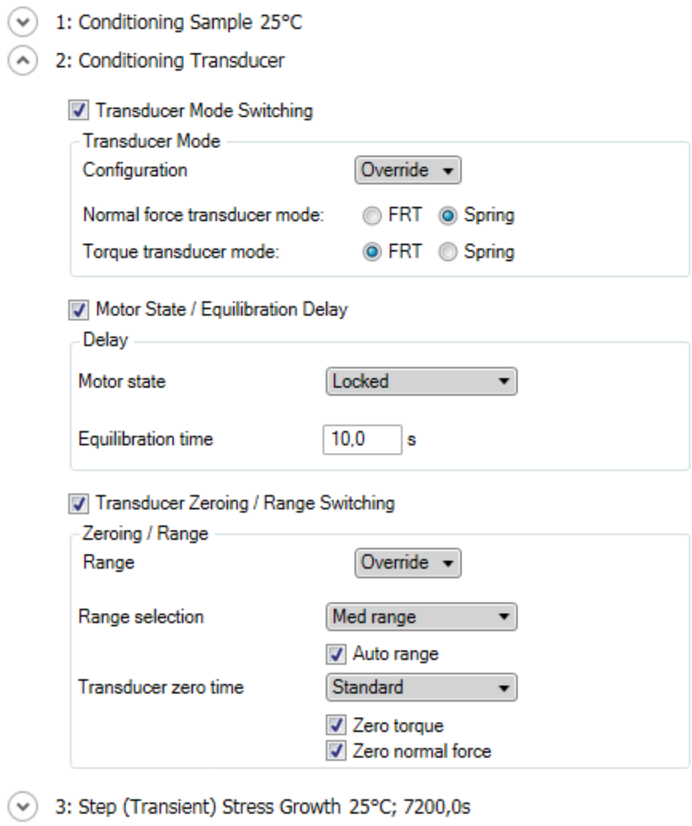

Figure B.1: Conditioning transducer step

A conditioning sample step is necessary to ensure the sample temperature is uniform and at the desired temperature at the beginning of the test. This step is also important to guarantee that the material has enough time to relax before the start of each test. Figure B.2 shows the conditioning sample step used to perform the rheometric experiments in this work.

In the conditioning sample step, the desired temperature is set. In this work, all tests were performed at 25°C. The "soak" time indicates the time needed for the material to reach the temperature chosen. The soak time may vary due to the type of material studied. This parameter was 10 minutes for the experiments performed for the gels, 5 minutes for air, and 30 minutes for oils. Regarding the latter, it is always recommended that more time is left for the temperature equilibrium.

The pre-shear option was selected for all tests done for the yield stress. First, the material was pre-sheared at a constant shear rate of 50 1/s for 60 seconds. Then, the material is left to rest for another 10 minutes, and this is indicated at the "Equilibration" time.

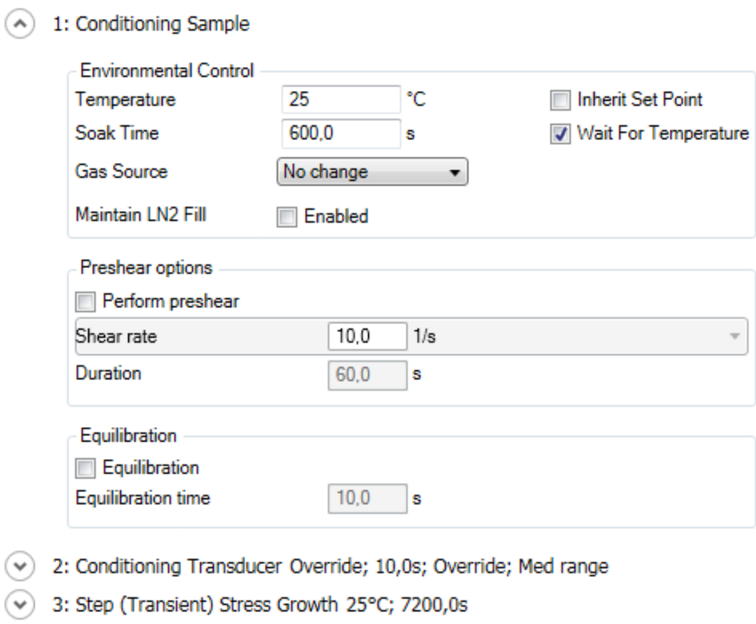

Figure B.2: Conditioning sample step